IDŐJÁRÁS

QUARTERLY JOURNAL
OF THE HUNGARIAN METEOROLOGICAL SERVICE

CONTENTS

VOL. 100 * NO. 4 * OCTOBER–DECEMBER 1996

IDŐJÁRÁS

Quarterly Journal of the Hungarian Meteorological Service

Editorial Office: P.O. Box 39, H-1675 Budapest, Hungary or
Gilice tér 39, H-1181 Budapest, Hungary
E-mail: gmajor@met.hu; Fax: (36-1) 290-7387
antal@met.hu

Subscription from customers in Hungary should be sent to the Financial Department of the Hungarian Meteorological Service, Kitaibel Pál u. 1, H-1024 Budapest

Abroad the journal can be purchased from the distributor: KULTURA, P.O. Box 149, H-1389 Budapest

IDŐJÁRÁS

Quarterly Journal of the Hungarian Meteorological Service
Vol. 100, No. 4, October–December 1996

ARPEGE/ALADIN: A numerical weather prediction model for Central-Europe with the participation of the Hungarian Meteorological Service

A. Horányi, I. Ihász and **G. Radnóti**

Hungarian Meteorological Service,
H-1525 Budapest, P.O. Box 38, Hungary

(Manuscript received 19 June 1995; in final form 10 October 1995)

Abstract—This paper intends to give a general description of the limited area numerical weather prediction model ARPEGE/ALADIN developed by a collaboration between Météo-France and some Central- and Eastern-European meteorological services (and also Morocco) including the Hungarian Meteorological Service (HMS). The model is a hydrostatic, spectral limited area model for dynamical adaptation at the limit of the hydrostatic approximation. The main characteristics of the model are discussed like the preparation of initial and lateral boundary conditions, the initialization method, the representation of the meteorological fields, the dynamics, the physics and the post-processing. The first experiences at HMS are discussed in the light of the one year quasi-operational application of the model. Finally, the possible future utilization for nowcasting purposes is mentioned.

Key-words: numerical weather prediction, spectral limited area model, dynamical adaptation, coupling, double-periodicization.

1. Introduction

The aim of this paper is to describe a new limited area model which is developed in collaboration with other Central- and Eastern-European countries and Morocco as well with French leadership. Nowadays in the operational numerical weather prediction practice two main intentions can be identified. The first is the improvement of the initial data for the models, using more measurements and more exact data assimilation methods. Due to the chaotic behaviour of the atmosphere without exact initial conditions, even a 'perfect' model could not provide a good forecast, therefore the improvement of the quantity (new type of data as Doppler radars, windprofilers etc.) and quality of initial data is of great importance. The second tendency is the improvement of

the models by enhancing their resolution and especially their physical parameterization package in order to have better models for the prediction of local weather phenomena. During the last 20 years, beside the global models, more meteorological services started to use limited area models for operational purposes (following the latter tendency), which are specialized for high resolution short range numerical weather prediction. Recently the Hungarian Meteorological Service (HMS) also applies operationally a limited area model adapted from the Swedish Meteorological and Hydrological Institute (*Dévényi et al.,* 1992). This model uses a resolution of 0.9 × 0.9 degrees with 12 vertical levels. The implementation of this model was a major milestone in the field of predicting local meteorological events for the Carpathian basin. However, the resolution of this model is still not satisfactory, especially if the ECMWF (European Centre for Medium Range Weather Forecasting) products (getting full ECMWF products became possible with the status of associated membership) are kept in mind with their similar resolution. The Hungarian Meteorological Service has realized the necessity to have a modern high resolution limited area model, so in 1990 an offer of Météo-France was accepted to participate in an international collaboration in the field of numerical weather prediction. The other countries joining the collaboration until now are Austria, Bulgaria, Croatia, Czech Republic, Morocco, Poland, Romania, Slovakia and Slovenia. The main purpose of this project was the development of the limited area counterpart of the global French numerical weather prediction model (ARPEGE). The main development phase of the project was finished at the end of 1992. For the entire 1993 the model was mainly used for research studies and after getting new financial fundings the model was quasi-operationally implemented in Toulouse starting from 31 May, 1994. This paper intends to give a detailed description of this model, which is developed with the participation of HMS and also to mention its potential future applications for numerical weather prediction purposes for our region.

2. Projects for model developments

The project ARPEGE/IFS is a collaboration between Météo-France and ECMWF in numerical weather prediction. The main goals of this collaboration were to develop efficient data assimilation tools (variational assimilation) and also to have numerical weather prediction models at every spatial and time scale (*Courtier et al.,* 1991). These ambitious goals were covered by one model family which is called IFS (Integrated Forecasting System) at ECMWF and ARPEGE (Action de Recherche Petite Echelle Grande Echelle — research at small and large scale) in France. The models are spectral hydrostatic global models (*Courtier* and *Geleyn*, 1988) with the corresponding initializations and preparations of initial fields. The French acronym indicates one of the most

important feature of the models to have variable resolution using the idea of *Schmidt* (1977). This means that the resolution changes over the whole sphere according to a stretching factor. In France the original idea was to use the ARPEGE global model for both synoptic and mesoscale purposes with the relevant choice of the stretching factor. The main advantage of this solution is to avoid the negative effect of the lateral boundary conditions between a high resolution domain and the coarser resolution area. However, stretching can't be increased infinitely to increase the resolution in a given area (and decrease it on the other side of the Earth), due to the fact that the spectral characteristics are broken after a limit stretching value. This statement means that for very high resolutions (near to meso-β scale) this solution can't be applied (*Caian* and *Geleyn*, 1995).

Hereafter the main elements of the ARPEGE/IFS model system are introduced. These elements can be activated by a properly chosen configuration number and they are as follows:

- 3D forecast model using the primitive equations of the atmosphere,
- variational assimilation (3D variational analysis and different options of 4D variational analysis),
- 2D forecast models (shallow water model, vorticity equation model, linear gravity wave model),
- Kalman filter and predictability studies,
- test of the adjoint models,
- test of the tangent linear models,
- calculation of eigenvalues and eigenvectors,
- objective analysis using optimal interpolation,
- sensitivity studies,
- geometrical transformations for the preparation of initial conditions of the models.

In 1990 Météo-France launched an initiative in order to start a collaboration with Central- and Eastern-European countries in numerical weather prediction. The proposal was directed towards the development of the limited area counterpart of the global spectral ARPEGE/IFS model system. The main objective of the project to be fulfilled was to develop a limited area model in the framework of the existing ARPEGE/IFS code for dynamical adaptation at the limit of the hydrostatic approximation. The ALADIN model is intended to be a version of the ARPEGE/IFS code system using as much as it is possible the already existing code and creating new modules only if it is unavoidable. From a practical point of view it means that the main part of the model existed even before the development was started. It is especially true for the main scientific part of the model (the grid-point calculations) which is so general and independent of any metric or geometry that it can be used without any

modifications also for limited area purposes. Dynamical adaptation stands for a system, where independent objective analysis isn't carried out for producing initial and lateral boundary conditions, only simple interpolation is performed starting from global ARPEGE fields. The target resolution is at around the limit of the hydrostatic approximation. Hereafter the main points (where the original system had to be modified) to be considered in the development of the model are reviewed:

- The consideration of the meteorological processes evolving outside the domain using coupling. The coupling is achieved by a relaxation technique, which ensures continuous transition between the internal and external part of the model domain.
- The geometric transformation of the spherical geometry onto the limited area in order to prepare the initial and lateral boundary conditions.
- The modification of the horizontal representation of the fields from spherical harmonics to full harmonic functions and taking into account all of its consequences (e.g. derivative calculations, spectral space computations).
- The development of digital filter dynamical initialization method.

The solution of these basic tasks allowed to create the limited area spectral model called ALADIN (Aire Limitee Adaptation Dynamique Developpement International — international development of a limited area model for dynamical adaptation) or ARPEGE/ALADIN referring to the mother system ARPEGE. After the development and refinement of the basic parts of the model some research topics were defined such as the application of the tangent linear and adjoint versions for sensitivity studies or the development of a non-hydrostatic version.

3. The general description of the model system ARPEGE/ALADIN

As it was mentioned before, ARPEGE/ALADIN is a hydrostatic, spectral limited area model. Recently for global numerical modelling spectral methods are generally used because of having certain advantages with respect to the traditional grid-point methods. Mostly these advantages are preserved in the case of limited area applications and they are summarized below:

- the possible simple and more accurate calculation of derivative fields,
- good description of the phase and amplitude of the meteorological fields,
- the horizontal and vertical dimensions are well separated allowing simplified conservation properties,
- easy and cheap implementation of semi-implicit time integration schemes,

- simple unaliasing condition due to the spectral truncation,
- the technique can be easily extended to variational developments,
- less disk space requirements due to the data storage in the form of spectral coefficients.

Taking into account these advantages *Machenhauer* and *Haugen* (1987) proposed the full harmonic expansion of the meteorological fields (which means that the fields must be double-periodic) in the case of spectral limited area applications. This solution was implemented for the ARPEGE/ALADIN model.

As far as the execution of the model system is concerned it is decomposed into three main steps. The first two preparatory steps provide climatological fields and initial and lateral boundary conditions over the limited area for the model integration. During the preparation of climatological fields using global climatological fields and the definition of the domain interpolation is carried out onto the limited area. The results of this operation are monthly average climatological fields for the given domain (*Cordoneanu,* personal communication). In the second phase similar interpolation is performed in order to obtain the initial and lateral boundary conditions for the limited area model. During this operation the analyses and the forecasts of the global model are interpolated to the target grid. The climatological fields, the initial and lateral boundary conditions are already double-periodic. This fact prevents further double-periodicization during the time integration of the model. After these preparations the heart of the model system, the integration of the non-linear hydrostatic model takes place. The main aspects of the integration are the dynamical initialization of the initial fields (using digital filters), the calculation of dynamical and physical tendencies using Eulerian or semi-Lagrangian semi-implicit time integration scheme, consideration of lateral boundary conditions through coupling, the creation of post-processed fields using internal post-processing.

In the following sections these major steps will be reviewed with special emphasis on the model part.

3.1 The preparation of initial and lateral boundary data

The double-periodic initial and lateral boundary conditions of model ALADIN are obtained by interpolation from global ARPEGE analyses and forecasts. The following sequence of operations (the order is of great importance) are performed: the transformation of global spectral fields from spherical harmonics to the collocation grid, horizontal interpolation, double-periodicization and afterwards vertical interpolations to the target geometry and finally transformation of the grid-point fields into full harmonics. The horizontal interpolation is done with the possibility to use a bilinear or a 12-point interpolation with cubic Lagrangian polynomials. The most important option running the

horizontal interpolations is the capability of using departures between the climatological mean values and the surface prognostic fields. This option ensures to have small scale details in the interpolated data. For the vertical interpolation a displacement of the planetary boundary layer (PBL) has been implemented in order to keep its structure as much as it is possible. For this method first an intermediate vertical system is created which is defined by a special combination of the characteristics of the input and target systems. The next step is the vertical interpolation from the input and intermediate systems to the target one using a weight function varying between zero and one and which ensures smooth transition in the PBL transition layer. Below this transition zone the results of the intermediate system are taken alone and above it only the original one is considered (*Bubnová et al.,* 1993).

Concerning the double-periodicization, it is an operation which makes the meteorological fields double-periodic (periodic in both direction of the plane). This operation is essential in order to be capable for performing Fourier transformations for the calculation of derivatives. The double-periodicization operator should also take care not to introduce undesirable numerical noises in the area of meteorological interest. As double-periodicization operator, cubic spline functions are used with subsequent Laplacian transversal smoothing with the following desirable features: continuous derivatives up to second order, isotropy and no unrealistic overshooting (*Batka,* personal communication).

Finally, after the double-periodicization and the direct spectral transformations all the necessary information is available (in the form of spectral coefficients) for the integration of the model. These are the three dimensional state variables of the model like temperature, wind components and specific humidity and two dimensional variables like surface pressure and orography. The necessary surface fields are surface and deep soil temperature, surface and deep soil relative moisture contents, snow cover, albedo, emissivity, land-sea mask, proportion of vegetation, roughness length, standard deviation, anisotropy and orientation of subgrid-scale orography.

3.2 Digital filter initialization

Due to the finer orography used by ALADIN and the noise unavoidably introduced by the interpolation from the global to limited area geometry, dynamical initialization of the prognostic fields is desirable even if the original information came from an initialized state. Therefore the time integration is preceeded by the dynamical initialization of the initial fields.

For ALADIN it was decided to implement the digital filter initialization method (*Lynch* and *Huang*, 1992) instead of adapting the non-linear normal mode initialization from the global model. The main purpose of the initialization is the removal of those fast propagating inertia-gravity waves from the initial conditions which would cause numerical instability at the beginning of the

integration. For the digital filters the main idea is filtering out the high frequency noises by considering the temporal Fourier series of the fields of interest and setting to zero the Fourier coefficients corresponding to high frequency waves and recompute the fields again. Then these fields will not contain high frequency spurious waves any more. It can be seen that the method is very simple, its coding is based on a very simple algorithm. On top of that the method is not sensitive to the formulation and the changes of the model and there are no convergence problems as for normal modes. The success of the utilisation of digital filters (with its various variants as recursive or non-recursive, diabatic or adiabatic, incremental or non-incremental filters) inspired its potential application also for the ARPEGE global system (*Ivanovici,* personal communication).

3.3 The vertical representation of the meteorological fields

The vertical coordinate to be used is the pressure based hybrid coordinate η following the orography as described by *Simmons* and *Burridge* (1981). The main feature of this coordinate is that at the bottom of the model it is terrain following and at the top it is pressure type coordinate. The vertical coordinate is defined by the following implicit relationship:

$$p(x,y,\eta,t) = A(\eta) + B(\eta)\,\pi(x,y,t)\,, \tag{1}$$

where η is the vertical coordinate, p is the pressure, π is the surface pressure and A and B are constants depending on the vertical levels. The η vertical coordinate varies between 0 and 1 (0 at the top and 1 at the bottom) and the following conditions are fulfilled:

$$A(1) = 0\,; \quad B(1) = 1\,; \quad B(0) = 0 \quad \text{and} \quad \frac{\partial \eta}{\partial p} > 0\,. \tag{2}$$

Therefore the vertical coordinate is defined by the constants A and B. This coordinate with a properly chosen vertical discretisation ensures the conservation of energy and angular momentum of the system (*Simmons* and *Burridge*, 1981). This main constraint was kept in mind while designing the vertical discretisation scheme. The model is vertically discretised into L layers. Between model levels layer boundaries ($L + 1$) are also defined. The model variables are naturally defined at model levels and fluxes and advecting vertical velocity at half levels. It is mentioned here that the Eq. (1) for the definition of the vertical coordinate is valid for half levels and the pressure values of the main levels can be computed from the half level values. The vertical discretisation is of great importance for the hydrostatic equation through its vertical integration.

3.4 The horizontal representation of the meteorological fields

The horizontal domain of ALADIN is decomposed into three regions which are shown in *Fig. 1*. These are as follows:

- Inner zone, which is in fact the domain of meteorological interest for adapting the larger scale forecast to a smaller scale orography or surface conditions. It is labelled by *C* as central zone.
- Intermediate zone (denoted by *I*), where the large scale solution is mixed together with the central zone solution. This zone is also called coupling zone or relaxation zone.
- Extension zone, which is considered for the spectral expansion. In this zone the fields are extended in agreement with the chosen basis function (these are the full harmonic functions). It is labelled with *E*.

The fields are geographically meaningful over the *C* and *I* zone, for the *E* zone those are expanded as a result of a purely mathematical operation.

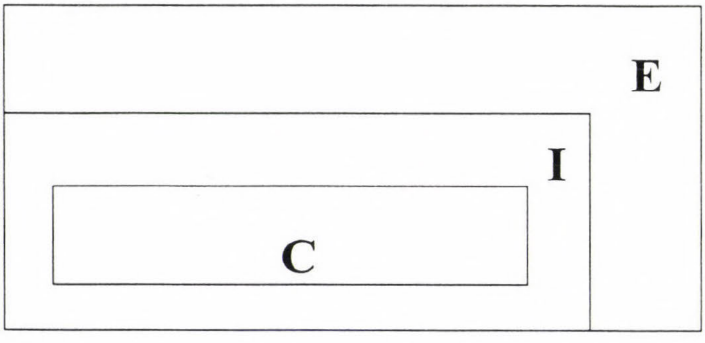

Fig. 1. The horizontal domain of ARPEGE/ALADIN. The *C* zone is the inner domain, the domain of meteorological interest. The *I* zone is the relaxation zone, where the coupling term is considered. The *E* zone is the extension zone, the region for double-periodicization.

Following the idea of *Machenhauer* and *Haugen* (1987) and considering an arbitrary *X* field its full harmonic expansion reads as:

$$X(x,y,\eta,t) = \sum_{m=-M}^{M} \sum_{n=-N}^{N} X_m^n(\eta,t)\, e^{im(2\pi/L_x)x}\, e^{in(2\pi/L_y)y}, \qquad (3)$$

where L_x and L_y are the horizontal wavelengths and X_m^n-s are the spectral coefficients corresponding to the given waves. The field X is expressed by the combination of different waves with different wavenumbers. This formulation

directly gives the truncated form, but from mathematical point of view the summation is of course infinite. It can be seen that the largest wavenumber considered in x direction is $M(2\pi/L_x)$ and in y direction it is $N(2\pi/L_y)$. It is clear from Eq. (3) that the calculation of the derivatives of X is rather simple knowing the spectral coefficients. These spectral coefficients can be calculated from the continuous form as:

$$X_m^n(\eta,t) = \frac{1}{JK} \sum_{j=0}^{J-1} \sum_{k=0}^{K-1} X(j,k,\eta,t)\, e^{-im(2\pi/J)j}\, e^{-in(2\pi/K)k}, \tag{4}$$

where J is the number of points along x and K is the number of points along y.

Eqs. (3) and (4) define the direct and inverse Fourier transformation between spectral and physical spaces. Inverse transforms are performed while going from spectral space to physical space and direct ones in the other direction. The transformations are decomposed into two steps for the two horizontal directions. The double-Fourier inverse transforms create the set of spectral coefficients and for every pair of waves there are four real coefficients. For the calculation of the coefficients in order to keep the isotropy the following constraint is considered:

$$\frac{n^2}{N^2} + \frac{m^2}{M^2} \leq 1, \tag{5}$$

where M and N are the maximum wavenumbers (these are chosen according to the size of the domain in the x and y direction, respectively). This expression defines the elliptic truncation, which has the same properties on the Cartesian plane as the triangular truncation of spherical harmonics on the sphere.

Another big advantage of the application of Fourier series is the fact that there exists a computationally efficient algorithm for transforming real fields. This algorithm is the Fast Fourier Transform (FFT) and utilizes the optimization possibilities of the trigonometrical functions (*Temperton*, 1979). In spectral models the existence of efficient spectral transformations is of great importance due to the fact that these transforms are performed at each timestep of the model.

Eqs. (3) and (4) involve $2M + 1$ and $2N + 1$ modes in spectral space and J and K points in physical space. Obviously, the number of waves and the number of points aren't independent parameters. Let us consider a field of a physical quantity, which is characterized by M modes in spectral or $2M$ points in physical space. When products of such fields are considered in physical space, information on wavenumber larger than M is created, i.e. if Eq. (4) is performed on the same $2M$ points the M waves aren't sufficient for describing

the given quantity due to the so called aliasing errors which might lead to nonlinear instability. Therefore in order to avoid aliasing, more points need to be defined for a given number of modes. The number of points depends on the highest order of product to be considered for solving the physical problem. In the case of ALADIN, the relationship between the number of points and waves is:

$$J \geq 3M + 1 \quad \text{and} \quad K \geq 3N + 1 . \tag{6}$$

Concerning the number of points to be chosen, there are also some constraints because of the optimal performance of FFT-s.

3.5 The equations of the nonlinear, hydrostatic model

The horizontal momentum equations on the sphere for ARPEGE (*Courtier et al.*, 1991) can be expressed as the acceleration of the individual particle is equal to the accelerations due to pressure gradient force, Coriolis force and due to diffusion and different parameterization processes. The physical parameterization package for the ALADIN model is kept the same as it is used for its global counterpart:

- complete and cheap radiation scheme (*Geleyn* and *Hollingsworth*, 1979; *Ritter* and *Geleyn*, 1992),
- vertical exchange calculations taking into account a planetary boundary layer and a surface layer based on the Louis scheme (*Louis et al.*, 1982),
- shallow convection parameterization (*Geleyn*, 1987),
- gravity wave drag based on the scheme of Boer (*Boer et al.*, 1984),
- Bougeault-type deep convection scheme (*Bougeault*, 1985),
- simplified Kessler-type scheme for the large scale precipitation,
- force-restore method for the soil hydrology.

Concerning the horizontal momentum equations over a limited area, ARPEGE/ALADIN is capable for integrating the primitive equations over an arbitrarily chosen limited area (the domain can be in any part of the Earth with well defined position), with the smoothest and most regular possible distribution of grid points. The traditional system of latitudes and longitudes provides such a regularity only in the vicinity of the equator or if it is conveniently projected on a plane. In the latter case the optimal projection highly depends on the location of the domain. By taking into account the above mentioned aspects during the preparatory phase of the model integration the rotation of the spherical coordinates or the three basic conformal projections (polar stereographic, Lambert, Mercator) or the combination of rotation and projection is available.

Concerning the rotation of the latitude-longitude coordinates, the goal of this operation is to roughly center the domain of interest over the new equator. This kind of transformation is also used for the HIRLAM model (*Gustafsson*, 1993). After investigating this option it turns out that a rotation of the Equator to the domain of interest followed by the Mercator projection is the only coherent way to handle the spherical metric of a portion of a sphere. The above mentioned three conformal projections can be merged into one using their map factor function and a constant parameter (K). When $K = 1$, then the polar stereographic projection is considered. For the Lambert projection K varies between 0 and 1 and for the Mercator one it is 0. Using the above mentioned projections the fundamental scalars (e.g. vorticity and divergence) and pseudo-scalars (e.g. kinetic energy) can be defined in the framework of the Cartesian geometry.

When projecting the momentum equations from the sphere to the plane, some terms containing the characteristics of the projections occur. These terms (curvature terms) can be expressed explicitly in terms of map factor function and kinetic energy.

The other equations to be considered are the hydrostatic equation, the thermodynamic equation and the continuity equation. All the governing equations used by ALADIN can be found in the Appendix.

3.6 The semi-implicit semi-Lagrangian time integration scheme

The time integration of the model includes a semi-implicit correction for fast-propagating processes independently of the application of semi-Lagrangian scheme. The semi-implicit correction allows a bigger timestep due to the removal of some fast-propagating waves taking into account the Courants-Friedrichs-Levy condition. For the Eulerian version the explicit leap-frog scheme reads as:

$$\frac{e^+ - e^-}{2\Delta t} = D(e), \tag{7}$$

where e is the given variable at time t, e^+ is at $t + dt$ and e^- is at $t - dt$. D refers to the expressions on the right hand side of the differential equation. The operator D describes different processes e.g. energy conversions, advection, wave propagation etc. Some of the processes are linear or well approximated by a linear (L) operator and excluding them from the operator D gives

$$\frac{e^+ - e^-}{2\Delta t} = D(e) + \beta L \left[\frac{1}{2}(e^+ + e^-) - e \right], \tag{8}$$

where β is the semi-implicit coefficient. Utilizing the linearity of L, Eq. (8) can be rewritten as

$$(I - \beta \Delta t L)\, e^{+} = e^{+}_{explicit} + \beta \Delta t L (e^{-} - 2e)\,. \qquad (9)$$

It can be seen that the price for the increase of the timestep with the removal of some fast waves is the inversion of the matrix on the left hand side. It is remarked that the terms occurring on the right hand side are generally called as the explicit part of the semi-implicit correction and these operations are performed in the grid-point space. The matrix inversion of the left hand side is computed in spectral space, because it involves the inversion of a Laplacian operator. This latter operation is called the implicit part of the semi-implicit correction.

It was decided for ALADIN to implement the semi-Lagrangian scheme for the further increase of the timestep with the removal of some fast-propagating waves. The applied scheme for the model is originated from the existing semi-Lagrangian scheme of ARPEGE, only some adjustment was done to the plane geometry and the limited area character was kept in mind. The main characteristics of the scheme are as follows (*Janousek,* personal communication):

- three dimensional semi-Lagrangian advection,
- 3-time level scheme with second order accuracy,
- fully interpolating version, with provision for future implementation of vertically non-interpolating version,
- upstream trajectories,
- wind-component based approach to the solution of momentum equations,
- approximation of trajectories by stream lines, using trilinear interpolation of wind components for trajectory construction,
- 32-point interpolation of the terms in the trajectory points,
- off-centering technique in order to avoid spurious resonant wave generation.

The application of semi-Lagrangian scheme and the necessity of grid-point calculations over the extension zone have a special interaction due to the treatment of the trajectories coming form the extension zone. If calculations are needed over the extension zone (when coupling is performed before the grid-point calculations) the computation of the trajectories at the edge of the $C + I$ zone is rather complicated, because taking into account the double-periodicity information about the top and bottom of the integration area is needed at the same time. This can be solved only in a very complicated manner due to the special organization of grid-point calculations. At the same time these calculations would be very superfluous, because of the unnecessary computations over the extension zone. If such a coupling strategy is chosen (and it is the case for ALADIN), where there is no need for calculation over the E

zone, the solution for the semi-Lagrangian scheme is much simpler. In that case the treatment of the external boundary of *I* zone (where trajectories might come from the extension zone) is based on the assumption that values of variables in extension zone are constant along the line perpendicular to the boundaries. According to the experiences, the errors occurring due to this assumption can be controlled with a proper choice of the width of the relaxation zone.

3.7 The coupling

The purpose of coupling is to impose the larger scale solution on a part of the domain taking into account the processes evolving outside the limited area. The coupling is also responsible for removing the artificial reflection and transmission of small scale waves on the boundaries of the domain of interest (*C* zone). Within the coupling zone (*I*) there is a smooth transition between the fields produced by the global model and those of ALADIN. This method is also considered as relaxation and can be described by the following formula (*Davies*, 1976):

$$X^c = (1 - \alpha) X^{bc} + \alpha X^{ls}, \tag{10}$$

where X^{bc} refers to values before coupling, X^{ls} refers to large scale values at the external edge of *I* zone and X^c corresponds to the values after the coupling. α is the relaxation coefficient, its value is 0 for the *C* zone, varies between 0 and 1 for the *I* zone and 1 for the *E* zone. The relaxation coefficients for the *I* zone are deduced from some special differentiable functions (*Janiskova,* 1994). Some specific aspects of the chosen coupling strategy are mentioned in *Radnóti* (1995).

3.8 The post-processing

During the model integration in specified time intervals some post-processed fields are created, which are as follows: post-processed prognostic variables, instantaneous fluxes (surface fluxes) and cumulated fluxes (precipitation fluxes). The normal post-processed file contains the albedo, deep soil temperature, emissivity, geopotential, land-sea mask, mean sea level pressure, orography, orography deviation, relative humidity, relaxation temperature, relaxation water, roughness, skin water, snow depth, soil moisture, specific humidity, surface temperature, temperature, vegetation, vertical velocity and wind fields. The three dimensional fields are generally represented on pressure levels, although there is an option to keep the original η levels. The instantaneous fluxes file contains the 2 m relative humidity, 2 m specific humidity, 2 m temperature, 10 m wind, total cloud cover, 2 m minimum and maximum temperature. The cumulated fluxes file contains the convective precipitation, stratiform precipita-

tion, radiative fluxes, surface fluxes, gravity wave drag momentum fluxes and turbulent momentum fluxes.

4. The quasi-operational model and its results

ARPEGE/ALADIN is quasi-operationally applied in Toulouse (at the forecast center of Météo-France on a CRAY-90 computer) for a domain over Europe. The orography of the domain can be seen in *Fig. 2.*

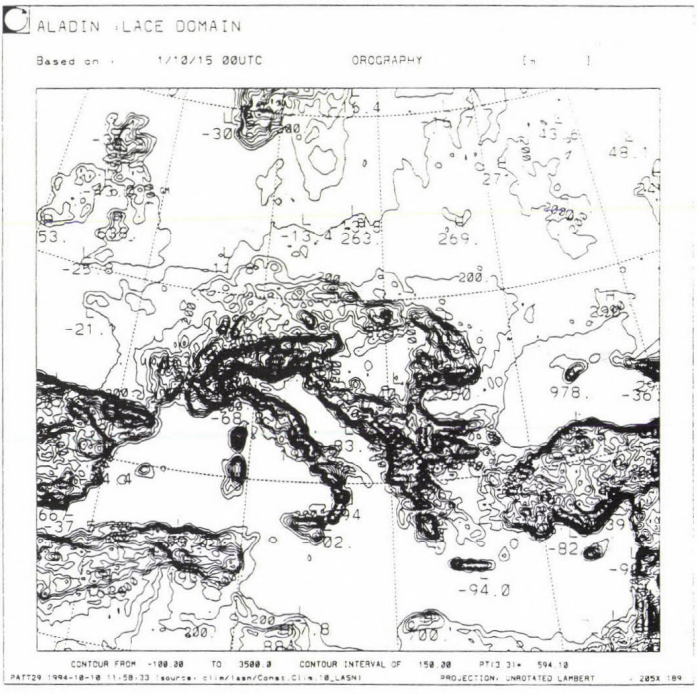

Fig. 2. The domain and the orography of the quasi-operational version of ARPEGE/ALADIN.

The main characteristics of the model are as follows:

- digital filter initialization,
- semi-implicit semi-Langrangian integration scheme with Asselin time filter,
- 432 seconds of timestep,
- circ. 18 km of horizontal resolution using 205 × 189 collocation grid points on Lambert projection,

- the domain size is around 3800 × 3400 km,
- 24 vertical levels (the lowest level is at 17 m and the highest is at 10 hPa),
- the boundary values are specified from ARPEGE and linearly interpolated with a 6 hour interval,
- the computational cost is around 4400 seconds CPU time for CRAY-98 (it roughly means 12 minutes execution time with 8 processors) for a 36 hours forecast.

The quasi-operational model is launched every day for 36 hours, starting from 00 UTC data and creates post-processed output fields every 6 hours. Some post-processed fields are disseminated to the participating countries in chart form via satellite. These charts are available for the bench-forecasters every day at around 04 UTC, so they can use them for operational purposes. The traditional meteorological forecast variables are available on pressure levels as geopotential, temperature, relative humidity, wind vector and also mean sea level pressure. In addition to this information, 10 m wind, wet bulb potential temperature, vertical velocity and precipitation forecasts are displayed on the disseminated maps.

5. Application of ALADIN products at HMS

The disseminated products of ALADIN (some examples can be seen in *Fig. 3*) are used in the daily operational suite at HMS. The receipt of these products are solved by MATRA satellite receivers. These machines were obtained from Météo-France in order to make possible the reception of numerical weather prediction products used in France. These are analyses and forecasts of French models (e.g. ARPEGE) and some alphanumeric telegrams used for aviation meteorology (like METAR or TAF messages). The data received by the MATRA station serve as a complement to the GTS information and these are particularly useful for aeronautical meteorological purposes, because it is able to complete automatically some flight plans and files for a predefined time. The application of this equipment was natural while the dissemination of ALADIN products was concerned. This device is able to decode the Tektronix files coming from Toulouse in order to produce meteorological charts. The charts can be visualized either on the screen or on the paper, however the ALADIN products are automatically plotted for the use of the forecaster on shift. As far as the application of the products is concerned three main fields can be identified: general forecast, aviation forecast and storm forecast. The general forecast provides predictions for the media and also some guidelines for the specialized forecasts and mostly uses the 12–36 hours ALADIN forecasts. The aviation and storm forecasts obviously utilizes shorter range forecasts due to

their nowcasting character. It is especially true for the storm forecast system at Lake Balaton (a MATRA receiver is also installed there), where up to date storm warnings have to be issued. In this field the possible further application of ALADIN products opens a new perspective with respect the dangerous quickly evolving small scale systems.

(a)

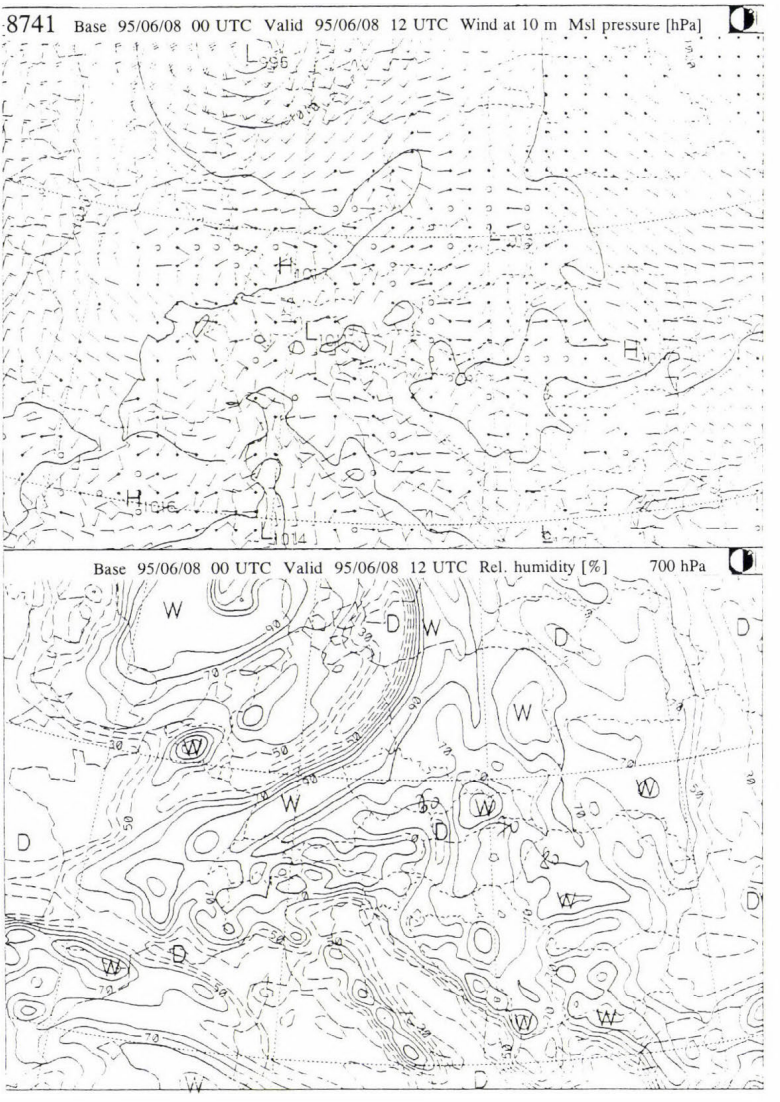

Fig. 3. A 12 hours forecast starting from 00 UTC, 08 June, 1995. (*a*) 10 m wind vector with mean sea level pressure (hPa) and relative humidity (%) at 700 hPa; (*b*) geopotential height (dam) with temperature (°C) at 500 hPa and vertical velocity (Pa/s) at 700 hPa.

Continued Fig. 3.

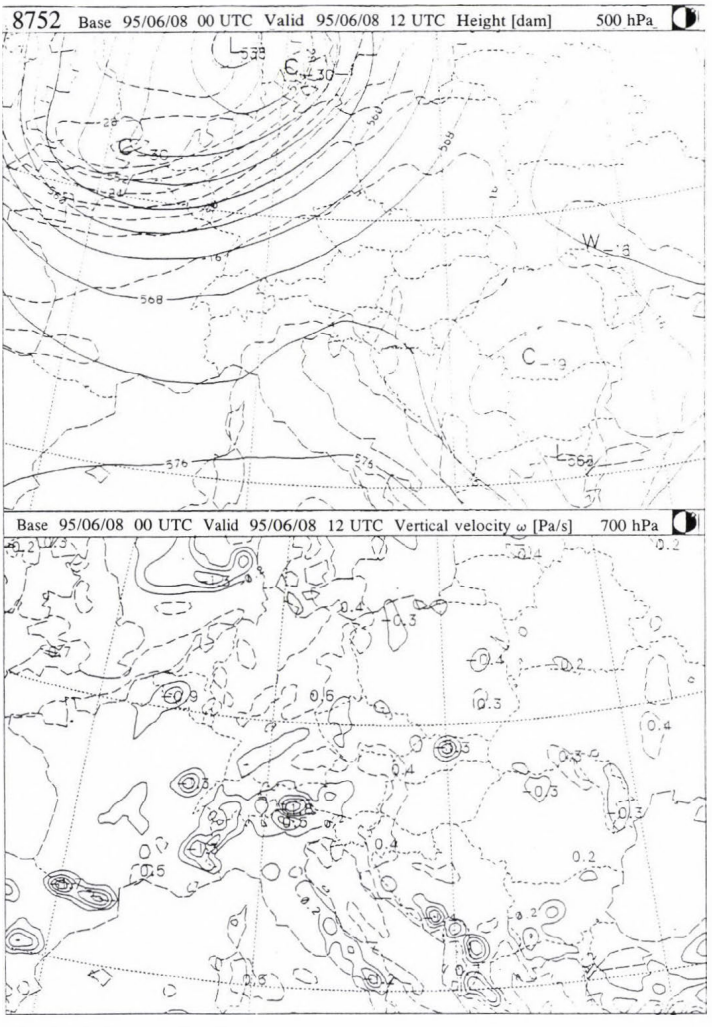

(b)

However at the moment, the technical facilities of the satellite dissemination do not make it possible to get the full meteorological information provided by the model (this fact is illustrated in *Fig. 4*), so further efforts are needed to get alphanumerical messages in order to benefit from the full horizontal and vertical resolution of the model. The first step towards this longer range goal is the receipt of electronic mail messages containing some vertical profiles in predefined stations of interest (Szombathely, Győr, Siófok, Pécs, Budapest, Szeged, Debrecen and Miskolc) over Hungary. These 'pseudo-TEMP' forecasts are displayed on workstations in traditional emagram form (see *Fig. 5*) and

those are especially useful for aviation meteorological purposes. In the near future it is planned to prepare the receipt of GRIB telegrams, which will allow us to utilize the full post-processed products of ARPEGE/ALADIN.

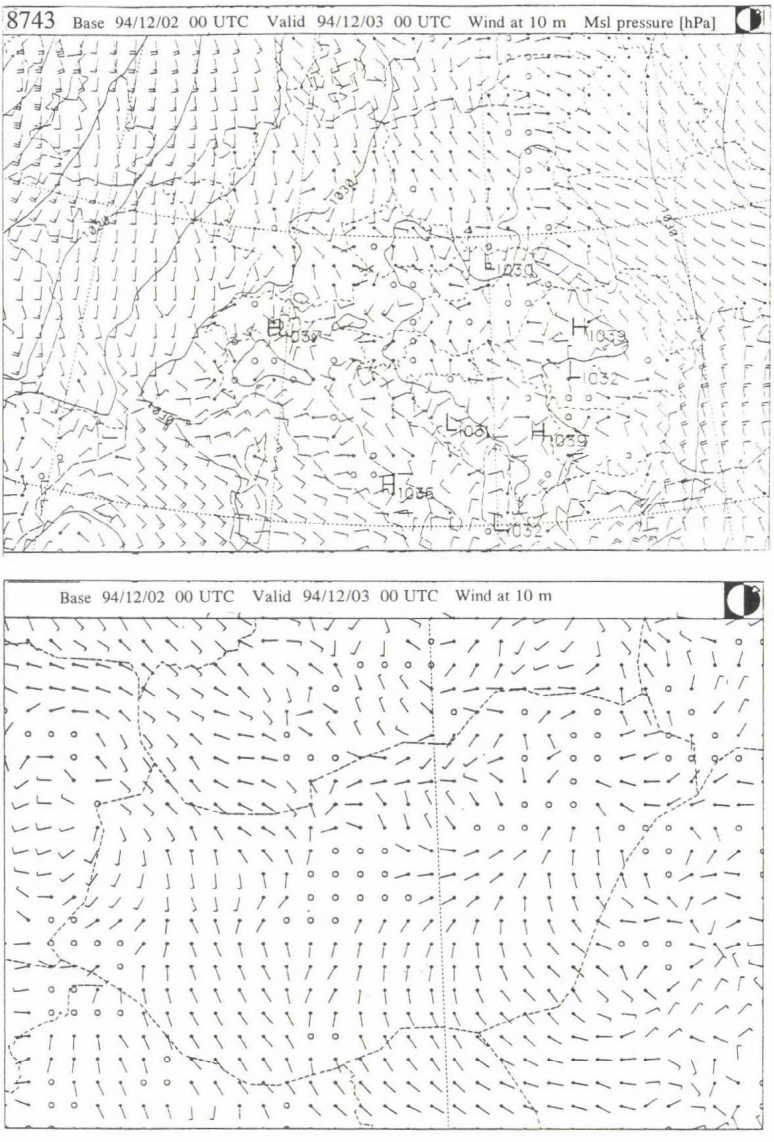

Fig. 4. Comparisons of 24 hours 10 m wind forecasts (based on 2 of December, 1994) in m/s over Hungary. (*a*) The traditional chart form used in the daily operational regime (every fourth gridpoints are displayed); (*b*) A zoom over Hungary displaying all gridpoints of the model.

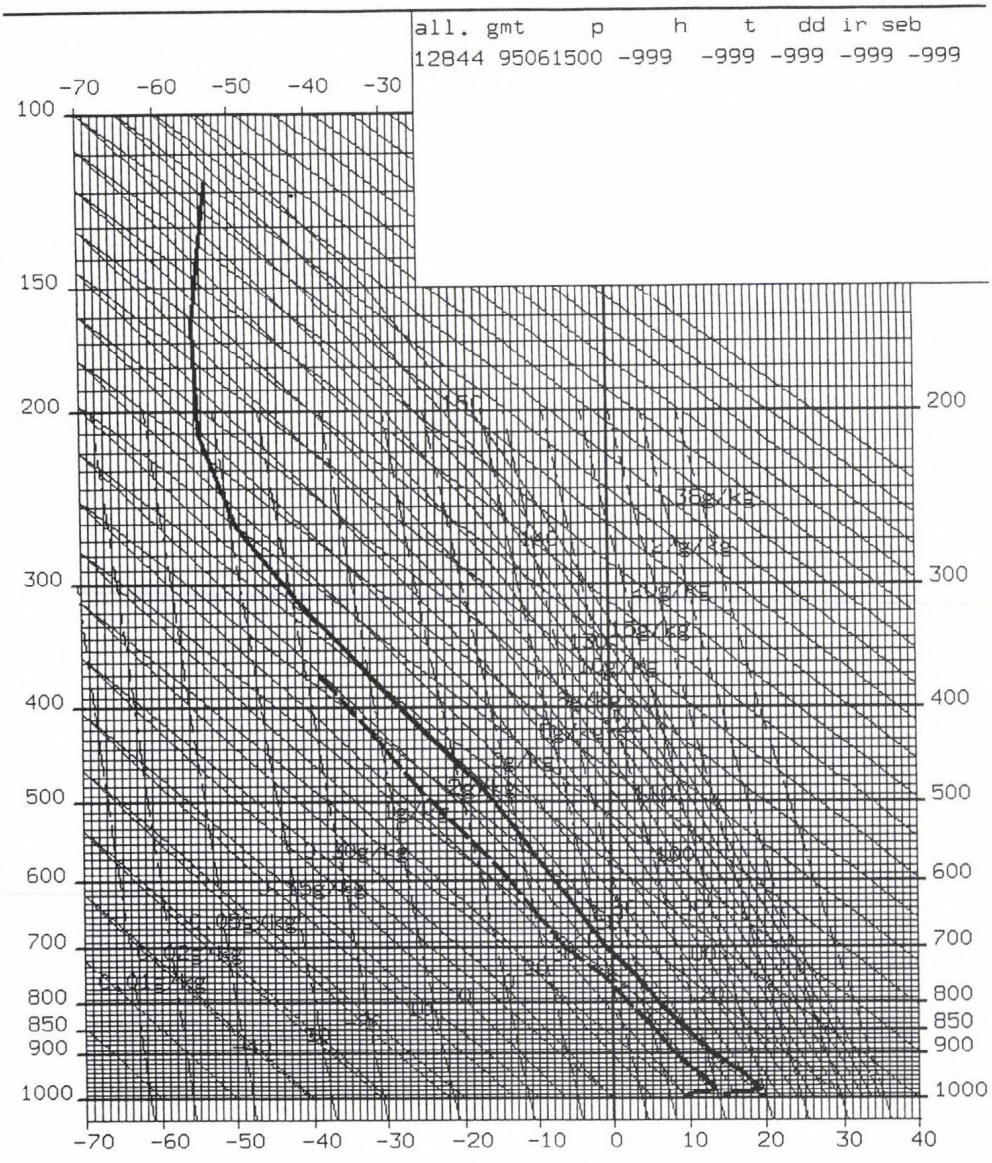

Fig. 5. An emagram prepared using 'pseudo-TEMP' message of ALADIN. A vertical profile of a 24 hours ALADIN forecast starting from 14 of June, 1995 over Budapest.

Concerning the evaluation of the ALADIN products, both objective and subjective verification is carried out. Before the quasi-operational start the basic validation of the model was performed by Czech, Polish and Hungarian

forecasters. In Toulouse the experts of Météo-France compute monthly verification scores (mean forecast error, standard deviation and root mean square error) with respect to SYNOP and TEMP observations and also comparison is done to the results of operational ARPEGE. The main conclusions of the objective verification are that ALADIN usually gave slightly worse scores than ARPEGE when it was compared to SYNOP observations for wind and slightly better for temperature fields. While ALADIN results are compared to TEMP observations for the lower part of the atmosphere the same conclusion can be drawn. These results are rather surprising according to the expectations. This weakness is probably linked to the exaggerated amount of surface and upper air drag in ALADIN with respect to ARPEGE. Ways to cure it are tested to find the best balance between the several factors contributing to the low level drag of the model.

In Budapest monthly subjective verifications over Hungary based on the disseminated charts are performed. Below some of the experiences will be summarized with respect to the one year utilization of ALADIN products in Hungary. Detailed case studies are out of scope of this paper, they are planned to be presented in another paper. Generally it can be said that the configuration of the meteorological objects (their mean sea level pressure, geopotential and temperature) is very well represented by ALADIN. It is especially useful in the case of mesoscale systems due to the fact that other models applied at HMS (e.g. UKMO or DWD models) have coarse resolution for predicting these regional events. Nevertheless, also sometimes weaknesses can be detected like the underestimation of 2 m temperature and the wind speed at 10 m. For the latter quantity it is interesting to note that practically overestimation never occurs even in the cases of very strong wind the model gives moderate values (see *Table 1*). For the temperature fields time by time overestimation can be noticed at 850 hPa and underestimation for the 500 hPa pressure levels. The mean sea level pattern is sometimes overestimated.

Table 1. Subjective evaluation of the 10 m wind speeds for September. The values are in percentage.

Time (hr)	Prediction		
	exact	high	low
06	70	-	30
12	17	-	83
18	53	-	47
24	77	-	23
30	59	-	41
36	15	-	85

One of the most important parameter to be considered is the precipitation. This variable caused most of the difficulty for the forecasters as far as its occurrence and quantity are concerned. At the first months the convective precipitation was strongly overestimated and due to this fact the frontal precipitation zones were hidden into the convective patterns. After the identification of this serious problem a modification of the convective precipitation parameterization scheme was implemented, which improved the results dramatically (*Table 2*). Recently the precipitation forecasts are much better (less overestimation and more correct forecasts), however this variable is still the most problematic one.

Table 2. Subjective verification of precipitation forecasts of ALADIN before (July) and after (September) the modification of the convection scheme. The values are in percentage.

The right forecast (first column) means those cases, when the position and the quantity of the forecast were correct. Second column: precipitation was forecasted, but didn't occur; third column: precipitation wasn't forecasted, but occurred; fourth column: precipitation was forecasted but to wrong place; fifth column: the position of the forecast was correct, but it was overestimated; sixth column: the position of the forecast was correct, but underestimated.

Time (hr)	Occurrence								Quantity			
	right		forec.: yes real: no		forec.: no real: yes		wrong place		over-estimation		under-estimation	
	Jul	Sep	Jul	Sep	Jul	Sep	Jul	Sep	Jul	Sep	Jul	Sep
06	35	40	24	7	32	27	4	10	-	-	5	17
12	22	57	35	13	8	10	16	10	5	3	14	7
18	24	53	27	13	-	7	13	20	14	-	22	7
24	18	70	50	7	-	3	9	7	18	7	5	7
30	37	57	32	57	18	27	7	3	3	-	3	13
36	16	54	43	4	-	23	9	8	14	8	18	4

6. Plans for the future

Concerning the future, the first objective is the full validation of the model in order to be capable for using it in operational way. To this end a systematic evaluation of the subjective and objective verifications will take place in order to discover the possibly existing weaknesses of the model.

Regarding the further development of the model there are ambitious objectives in that respect. Concerning the objective analysis and data assimilation recently the objective analysis scheme based on optimal interpolation is adapted from the ARPEGE system to ALADIN (in the framework of the French-Moroccan collaboration), however its full validation is not yet finished.

In the long term the implementation of variational assimilation schemes is planned. The first step towards this goal is the development of the tangent linear and adjoint versions of the model. The already existing adjoint version of the doubly-periodic version is used for sensitivity studies for the better understanding of the dynamics of frontal waves (*Horányi* and *Joly*, 1994). Regarding the dynamics of the model the improvement of the semi-Lagrangian scheme is of great importance. First of all a two-time level scheme is under implementation and later a more exact CUD-5 (compact upwind differencing) interpolation will be applied (*Tolstykh,* 1994, 1995). Another essential development is the creation of the non-hydrostatic version of the model. This work is based on the idea of *Laprise* (1992) introducing the hydrostatic pressure as vertical coordinate. This idea made it possible to transform the hydrostatic model into the non-hydrostatic one without deeply changing its basic structure (*Bubnová et al.*, 1995). The first results of the non-hydrostatic model are encouraging, which give a hope of its longer range operational applications. The climate version of the model is also under development and it is intended to participate in climate research projects by running ALADIN in climate mode.

Finally, it has to be mentioned that there is an international collaboration between Central-European countries (the participants are Austria, Croatia, Czech Republic, Hungary, Slovakia, and Slovenia) in order to establish a computer center where ALADIN can be launched operationally for the short range weather prediction purposes of the participating countries. This project is strongly supported by Météo-France, who made it possible to participate in the ALADIN project and allowed to use their computer power in the quasi-operational application of the model as well.

Acknowledgements—We would like to thank the whole staff of Météo-France in Toulouse for their hospitality and supports during the authors' stays in Toulouse. We are particularly grateful to the project leaders *Jean-Francois Geleyn*, *Alain Joly* and *Joel Hoffman* and also to *Emmanuel Legrand*. We also thank all ALADIN members for their contributions to the common work and among them *Sylvie Malardel*, who helped especially in practical questions. Furthermore, we would like to thank all Hungarian forecasters, who contributed to the work in some extent: *Imre Bonta, Szilvia Jenki* and *Ágnes Takács*. We are grateful for the support of the direction of HMS concerning the ALADIN project and it is a great pleasure to acknowledge the generous support of *Dr. Dezső Dévényi* and his particularly useful comments on the manuscript of the paper.

The ALADIN project was supported by different funds like the MICECO program, by the European Community, by the French Ministere de l' Enseignement Superieur et de la Recherche and also by the bilateral program called Balaton.

References

Boer, G.J., Mc Farlane, N.A., Laprise, R., Henderson, J.D. and *Blanchet, J.P.*, 1984: The Canadian Climate Centre spectral atmospheric general circulation model. *Atmos. Ocean 22,* 397-429.

Bougeault, Ph., 1985: Parameterization of cumulus convection for GATE. A diagnostic and semi-prognostic study. *Mon. Wea. Rev. 113,* 2108-2121.

Bubnová R., Horányi, A. and *Malardel, S.* 1993: International project ARPEGE/ALADIN. *EWGLAM Newsletter* 22, 117-130.

Bubnová, R., Hello, G., Benard, P. and *Geleyn, J.-F.*, 1995: Integration of the fully elastic equations cast in the hydrostatic pressure terrain-following coordinate in the framework of the ARPEGE/ALADIN NWP system. *Mon. Wea. Rev. 123,* 515-535.

Caian, M. and *Geleyn, J.-F.*, 1995: Some limits to the variable mesh solution and comparison with the nested LAM one. Submitted to *Quart. J. Roy. Meteorol. Soc.*

Courtier, Ph., Freydier, C., Geleyn, J.-F., Rabier, F. and *Rochas, M.*, 1991: The Arpege project at Météo-France. *Note de travail interne 'ARPEGE'.*

Courtier, Ph. and *Geleyn, J.-F.*, 1988: A global numerical weather prediction model with variable resolution: Application to shallow-water equations. *Quart. J. Roy. Meteorol. Soc. 114,* 1321-1346.

Davies, H.C., 1976: A lateral boundary formulation for multi-level prediction models. *Quart. J. Roy. Meteorol. Soc. 102,* 405-418.

Dévényi, D., Horányi, A., Ihász, I. and *Radnóti, G.*, 1992: Recent limited area modelling activities in Hungary. *EWGLAM Newsletter, 1992,* 47-50.

Geleyn, J.-F. and *Hollingsworth, A.*, 1979: An economical analytical method for the computation of the interaction between scattering and line absorption of radiation. *Beitr. Phys. Atmosph. 52,* 1-16.

Geleyn, J.-F., 1987: Use of a modified Richardson number for parameterizing the effect of shallow convection. *J. Meteor. Soc. Japan, Special NWP symposium issue,* 141-159.

Gustafsson, N. (ed.), 1993: HIRLAM 2 final report. *Technical report, c/o SMHI, S-601 76 Norrkoping, Sweden,* No. 9.

Horányi, A. and *Joly, A.*, 1994: Sensitivity studies using the doubly-periodic version of ARPEGE/ALADIN. *Abstract to the Second Workshop on Adjoint Applications in Dynamic Meteorology, 2-6 May, 1994, Visegrád, Hungary.*

Janiskova, M. 1994: Study of coupling problem. *Note ALADIN,* No. 1.

Laprise, R., 1992: The Euler equations of motion with hydrostatic pressure as an independent variable. *Mon. Wea. Rev. 120,* 197-207.

Louis, J.-F., Tiedke, M. and *Geleyn, J.-F.*, 1982: A short history of the PBL parametrization at ECMWF. *Proc. of the ECMWF workshop on planetary boundary layer parametrization, Reading, 25-27 Nov, 1981,* 59-80.

Lynch, P. and *Huang, X.Y.*, 1992: Initialization of the HIRLAM model using a digital filter. *Mon. Wea. Rev. 120,* 1019-1034.

Machenhauer, B. and *Haugen, J.E.*, 1987: Test of a spectral limited area shallow water model with time-dependent lateral boundary conditions and combined normal mode/semi-Lagrangian time integration schemes. In *Workshop Proceedings: Techniques for horizontal discretization in numerical weather prediction models; ECMWF, 2-4 November 1987,* 361-377.

Radnóti, G., 1995: Comments on: A spectral limited-area formulation with time-dependent boundary conditions applied to the shallow-water equations. *Mon. Wea. Rev. 123,* 3122-3123.

Ritter, B. and *Geleyn, J.-F.*, 1991: A comprehensive radiation scheme for numerical wether prediction models with potential applications in climate simulations. *Mon. Wea. Rev. 120,* 303-325.

Schmidt, F., 1977: Variable fine mesh in spectral global model. *Beitr. Phys. Atmos. 50,* 211-217.

Simmons, A. and *Burridge, D.*, 1981: An energy and angular momentum conserving vertical finite-difference scheme and hybrid vertical coordinates. *Mon. Wea. Rev. 109,* 2003-2012.

Temperton, C., 1979: Fast Fourier Transforms on Cray-1. *ECMWF internal report, 21.*

Tolstykh, M.A., 1994: Application of fifth-order compact upwind differencing to moisture transport equation in atmosphere. *J. Comput. Phys. 112,* 394-403.

Tolstykh, M.A., 1995: The response of the variable resolution semi-Lagrangian NWP model to the change of horizontal interpolation. Submitted to *Quart. J. Roy. Meteorol. Soc.*

APPENDIX

The governing equations of the model

According to the possible projections used by the model the horizontal momentum equations over the plane reads as follows:

$$\frac{\partial u}{\partial t} = \nu\varsigma - \nu\nabla^u \nu - u\nabla^u u - (u^2 + \nu^2)\, C_u(\varphi,\lambda) - \dot{\eta}\frac{\partial u}{\partial \eta} + f\nu - RT\nabla^u \ln p - \nabla^u \Phi - F^u$$

and

$$\frac{\partial \nu}{\partial t} = -\nu D - u\nabla^u \nu + \nu\nabla^u u - (u^2 + \nu^2)\, C_\nu(\varphi,\lambda) - \dot{\eta}\frac{\partial \nu}{\partial \eta} - fu - RT\nabla^\nu \ln p - \nabla^n \Phi - F^\nu, \tag{A.1}$$

where u and ν are the wind components, R is the gas constant, T is the temperature, f is the Coriolis parameter, Φ is the geopotential and ∇^u and ∇^ν denote the physical component of the gradient of a given field. D and ς are the divergence and vorticity, C_u and C_ν are the curvature terms and F^u and F^ν represent the forcing terms or in other words all the terms which are described by the physical processes of the model. The most important physical processes are the vertical turbulent diffusion, vertical exchange of momentum due to convection, vertical transport of momentum due to unresolved gravity waves generated by the small scale changes of the orography, the tendency resulting from momentum transport by falling precipitation, radiative budget, heating or cooling due to condensation of rain in stratified or convective clouds, evaporation of rain and all processes described by considering two or three phases of water.

The hydrostatic equation reads as:

$$\frac{\partial \Phi}{\partial \eta} = -\frac{RT}{p}\frac{\partial p}{\partial \eta}. \tag{A.2}$$

The mass conservation is expressed by the continuity equation, although for ARPEGE there is a possibility for the mass not to be conserved. In the latter case the mass changes are controlled by the precipitation-evaporation budget. Nevertheless, considering the total mass conservation (when the precipitating rain is replaced by air) the continuity equation reads as

$$\frac{\partial}{\partial t}\left[\frac{\partial p}{\partial \eta}\right] = -\nabla\left[V\frac{\partial p}{\partial \eta}\right] - \frac{\partial}{\partial \eta}\left[\dot{\eta}\frac{\partial p}{\partial \eta}\right], \tag{A.3}$$

where V denotes the horizontal wind vector.

If this equation is vertically integrated over the whole depth of the model atmosphere and suitable boundary conditions are taken into account, the evolution equation of the surface pressure can be obtained:

$$\frac{\partial \pi}{\partial t} = -\int_0^1 \nabla \left[V \frac{\partial p}{\partial \eta} \right] d\eta \,. \tag{A.4}$$

At an arbitrary η level using the definition of the vertical coordinate

$$\frac{\partial}{\partial t} \left[\frac{\partial p}{\partial \eta} \right] = \frac{dB(\eta)}{d\eta} \frac{\partial \pi}{\partial t} \tag{A.5}$$

can be deduced and integrating it from the top of the model atmosphere down to level η, one gets the advecting vertical velocity

$$\left[\dot{\eta} \frac{\partial p}{\partial \eta} \right] = -B(\eta) \frac{\partial \pi}{\partial t} - \int_0^\eta \nabla \left[V \frac{\partial p}{\partial \eta} \right] d\eta \,. \tag{A.6}$$

Finally by using the previous equations the pressure vertical velocity can also be expressed:

$$\omega = \frac{\partial p}{\partial t} + (V \nabla) p + \left[\dot{\eta} \frac{\partial p}{\partial \eta} \right] = B(\eta) V \nabla \pi - \int_0^\eta \nabla \left[V \frac{\partial p}{\partial \eta} \right] d\eta \,. \tag{A.7}$$

The thermodynamical energy equation can be written as:

$$\frac{\partial T}{\partial t} = -V \nabla T - \dot{\eta} \frac{\partial T}{\partial \eta} + \frac{RT}{c_p} \frac{\omega}{p} \,. \tag{A.8}$$

It is noted that for the calculation of gas constant and specific heat the humidity content of the atmosphere must also be considered.

IDŐJÁRÁS

Quarterly Journal of the Hungarian Meteorological Service
Vol. 100, No. 4, October–December 1996

A statistical model based on multiple regression applied to the prediction of air particle concentrations in the atmosphere

A. Boix[1], J. Mateu[2], M. M. Jordán[1] and T. Sanfeliu[1]

[1]*Departement de Ciencies Experimentals, Universitat Jaume I, Campus de Borriol, 12080 Castellón, Spain.*
[2]*Departament de Matematiques, Universitat Jaume I, Campus de Penyeta Roja, 12071 Castellón, Spain.*

(Manuscript received 15 May 1995; in final form 14 September 1995)

Abstract—A study of the statistical correlation was carried out between the air particle concentrations collected at two strategic points in the area of Castellón, using local weather parameters (wind speed, direction and air temperature). One of the stations was situated in Grao of Castellón, on the coast in the vicinity of an important industrial complex which houses an electricity generating plant, a petro-chemical plant and various auxilliary industries. The second station was installed in the city centre, where it is subject to diverse emissions of an urban nature (domestic heating systems, vehicles, construction work, infrastructural factors, etc.)

This paper intends to establish the most determinant variables of the air particle concentrations from each of the sample stations by means of the application of linear regression models. The independent variables of the first model are the normalized temperature, wind speed and direction data.

Differences were observed between the sample stations. At Grao station, the most influential meteorological parameter on air particle concentrations was wind direction, whilst wind speed and temperature were of secondary importance. However, in the case of the city centre station, the most important variable is undoubtedly the wind speed.

The second model consists of the previous model plus the SO_2 concentration level measured at the sample station itself. The importance of SO_2 as an independent variable was clearly seen at the city centre station (Herrero), since the multiple regression coefficient calculated for this second model, was larger. Therefore, after wind speed, SO_2 is seen to be the second determining factor in the air particle concentrations measured at Herrero station.

However, the SO_2 measured at the station located in Grao is not at all decisive for the proposed linear regression equation, being of much lesser importance than local meteorological parameters.

Key-words: statistical model, particle concentration, Spain, multiple regression.

1. Introduction

Within the study of atmospheric pollution, air pollution by air particles deserves a special mention for various reasons: it increases atmospheric opacity and reduces visibility, it enters the respiratory system, and it can act synergetically by increasing the toxic effects of other pollutants, etc.

The main anthropogenic sources of air particles are the manufacture of inorganic materials for use in the building industry (the production of cement, plaster, building materials, ceramics, etc.), extraction industries (mines and quarries) and public works. Other sources include combustion processes, residues proceeding from industries involving polishing or grinding of surfaces or the petrochemical industry. The true composition depends on the origin of the air particles. Air particles of an edaphic nature are principally composed of calcium, aluminium and silicate, elements which are common to mineral soils. Additionally, the smoke emanating from any combustion process gives rise to large quantities of suspended air particles. Secondary air particles are formed in the atmosphere from chemical compositions such as ammoniac salts, sulphates and nitrates.

Experimental evidence demonstrates that there exists a pronounced relationship between wind and the presence of solids in suspension in the atmosphere, be it in an urban or rural environment. *Boix* (1992), in a study carried out in the area of Castellón, noted that wind speed has a directly influence on the concentrations of air particles. In a study carried out in Brussels, *Hallez et al.* (1984) show a marked exponential relationship between wind and the presence of particles in suspension. Air particles can cause a wide range of material damage. *Matyniak* (1989) calculated the distribution of SO_2 concentrations in the air over Poland. Physical aspects of the atmospheric aerosol were described by *Jaenicke* (1984) in relation with some climatic effects. *Horvath et al.* (1989) determined, at up to eleven location in the town of Vienna, the mass size distribution of the aerosol. Many authors have undertaken studies of these effects, such as Graedel's study (*Graedel* and *Mcgill*, 1986) of the degradation of buildings and Del Monte and Leysen's specific study (*Del Monte*, 1987; *Leysen*, 1989) of their effect on monuments. Air particles accelerate the process of corrosion, especially in the case of compositions containing sulphur. The effects of air particles on plant life have been studied by Harrison (*Harrison et al.*, 1989), principally the decrease in photosynthesis caused by impeding the penetration of the necessary quantities of sunlight, and therefore inhibiting growth. Studies have also appeared dealing with the influence of air particles on public health (see *Rondia* and *Closset,* 1985; *Liu et al.*, 1988). Air particles enter the human body almost exclusively through the respiratory system, and it is this which is most readily affected. *Lipnick* (1991) defined a mathematical relationship between chemical structure and toxicity using statistical models.

Castellón, a Spanish town situated on the Mediterranean coast, has two important nuclei of inhabitants, the Grao area situated at the coast and the town proper situated some 3 km inland to the west. The town centre is little affected by emissions into the atmosphere from the large industrial centres. Pollution there is ostensibly the product of vehicle and domestic heating emissions, as well as particle emissions caused by urban construction and works.

Without question, the Grao of Castellón is one of the most important industrial areas situated locally. It includes a petrochemical complex and power station. Other important industrial areas in the province are Almazora, Villarreal, Nules, Alcora and Onda, which together constitute one of the most important concentrations of ceramic tile industry in the world.

Two sampling sites were established in the following colleges: Herrero (in the center of the city) and Grao de Castellón. The geographic location of these sites can be found on the map accompanying this study (*Fig. 1*). In each of these sampling sites daily readings of sulphur dioxide and particle concentration levels were taken throughout 1993. Measurements were taken every 24 hours. Furthermore, data relating to direction and speed of wind and air temperature was collected at a site located in El Mijares Industrial Estate (see map).

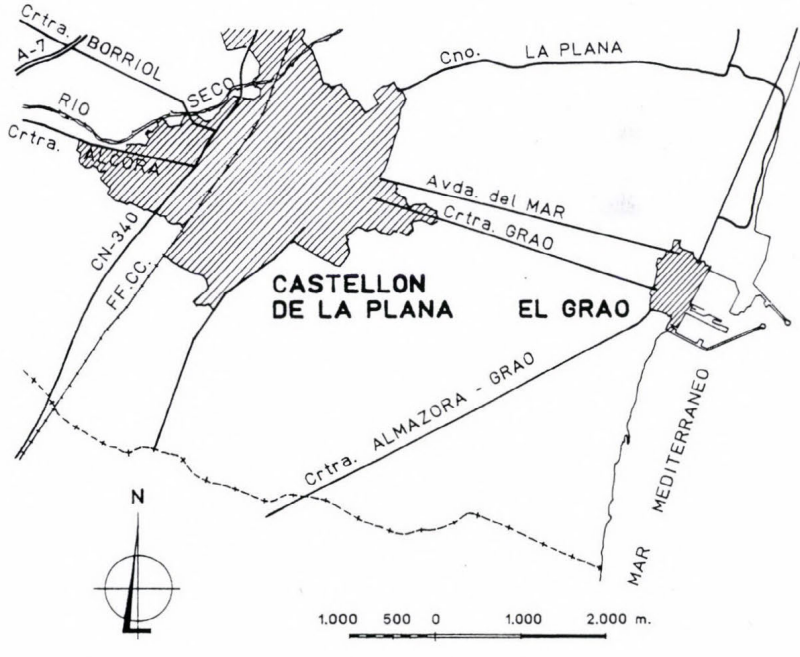

Fig. 1. Geographic location of the sampling sites.

2. *Experimental*

The samples taken provide data representing atmospheric pollution by SO_2 and particles in suspension. They were gathered using an MCV low volume detector of the type CPV-8 D/A, a model designed to detect sulphur dioxide and smoke (particle size < 11 μm), and with eight separate sampling periods. Samples were taken at the rate of 3 m^3/minute, and the filter papers were of 7 cm diametre Whatman No. 1. Sampling was done over a 24 hour period.

The technique used in determing the levels of emission of particles in suspension was that known as high volume sampling. SO_2 emission levels were determined using Thorina technical analysis.

The hourly data for wind speed and direction were obtained using a Fuess 90z-22E anemocinemograph which permitted the permanent register of wind data, its intensity and direction. The sensory devices of the anemocinemograph include a wind direction vane and an anemometre housing for measuring intensity. Measurements can be transmitted electrically. The range of wind intensity readings is between 0–40 m/s. The corresponding inscription needle responds electronically in one second.

3. *Statistics*

3.1 Multiple regression models

Multiple linear regression extends bivariate regression by incorporating multiple independent variables. The model can be expressed as:

$$Y_i = \beta_0 + \beta_1 X_{1i} + \beta_2 X_{2i} + \ldots + \beta_p X_{pi} + e_i \, .$$

The notation X_{pi} indicates the value of the pth independent variable for case i. The β terms are unknown parameters and the e_i terms are independent random variables that are normally distributed with mean 0 and constant variance σ^2. The model assumes that there is a normal distribution of the dependent variable for every combination of the values of the independent variables in the model (*Anderson*, 1984; *Draper* and *Smith*, 1981).

When working with several independent variables, it is important to calculate a correlation matrix for all variables. Remember that the correlation coefficient is a measure of the linear association between two variables. Particularly note that any large intercorrelations between the independent variables can substantially affect the results of multiple regression analysis (*Hoskuldsson*, 1988).

The F test associated with the analysis of variance table is a test of the null hypothesis that $\beta_1 = \beta_2 = \ldots = \beta_p = 0$. In other words, it is a test of whether

there is a linear relationship between the dependent variable and the entire set of independent variables. In multiple regression, the coefficients labeled B are called *partial regression coefficients* since the coefficient for a particular variable is adjusted for other independent variables in the equation.

It is also inappropriate to interpret the B's as indicators of the relative importance of variables. The actual magnitude of the coefficients depends on the units in which the variables are measured. Only if all independent variables are measured in the same units are their coefficients directly comparable. When variables differ substantially in units of measurement, the sheer magnitude of their coefficients does not reveal anything about relative importance. One way to make regression coefficients somewhat more comparable is to calculate *Beta weights*, which are the coefficients of the independent variables when all variables are expressed in standardized (Z-score) form. The Beta coefficients can be calculated directly from the regression coefficients using

$$BETA_k = B_k \left(\frac{S_k}{S_y} \right),$$

where S_k is the standard deviation of the kth independent variable.

Another way of assessing the relative importance of independent variables is to consider the increase in R^2 when a variable is entered into an equation that already contains the other independent variables. This increase is $R^2_{change} = R^2 - R^2_{(i)}$, where $R^2_{(i)}$ is the square of the multiple correlation coefficient when all independent variables except the ith are in the equation. A large change in R^2 indicates that a variable provides unique information about the dependent variable that is not available from the other independent variables in the equation. The signed square root of the increase is called the *part correlation coefficient*. It is the correlation between Y and X_i when the linear effects of the other independent variables have been removed from X_i. If all independent variables are uncorrelated, the change in R^2 when a variable is entered into the equation is simply the square of the correlation coefficient between that variable and the dependent variable. The square of the part coefficient tells only how much R^2 increases when a variable is added to the regression equation. It does not indicate what proportion of the unexplained variation this increase constitutes. If most of the variation had been explained by the other variables, a small part correlation is all that is possible for the remaining variable. It may therefore be difficult to compare part coefficients.

A coefficient that measures the proportional reduction in variation is

$$P_{\eta^2} = \frac{R^2 - R^2_{(i)}}{1 - R^2_{(i)}}.$$

The numerator is the square of the part coefficient; the denominator is the proportion of unexplained variation when all but the *i*th variable are in the equation. The signed square root of P_{η^2} is the *partial correlation coefficient.* It can be interpreted as the correlation between the *i*th independent variable and the dependent variable when the linear effects of the other independent variables have been removed from both X_i and Y. Since the denominator of P_{η^2} is always less than or equal to 1, the part correlation coefficient is never larger in absolute value than the partial correlation coefficient.

The null hypothesis that the true population value for the change in R^2 is 0 can be tested using

$$F_{change} = \frac{R_{change}{}^2 (N - p - 1)}{q(1 - R^2)},$$

where N is the number of cases in the equation, p is the total number of independent variables in the equation, and q is the number of variables entered at this step. Sometimes, this is referred to as a partial F test. Under the hypothesis that the true change is 0, the significance of the value labeled F_{change} can be obtained from the F distribution with q and N-p-1 degrees of freedom.

The hypothesis that the real change in R^2 is 0 can also be formulated in terms of the β parameters. When only the *i*th variable is added in a step, the hypothesis that the change in R^2 is 0 is equivalent to the hypothesis that β_i is 0. The F value printed for the change in R^2 is the square of the t value displayed for the test of the coefficient. When q independent variables are centered in a single step, the test that R^2 is 0 is equivalent to the simultaneous test that the coefficients of all q variables are 0.

When highly intercorrelated independent variables are included in a regression equation, results may appear anomalous. The overall regression may be significant while none of the individual coefficients are significant. High correlations between independent variables inflate the variances of the estimates, making individual coefficients quite unreliable.

Including irrelevant variables to the equation increases the standard errors of all estimates without improving prediction. On the other hand, it is important not to exclude potentially relevant independent variables. It is needed to use a procedure for selecting variables. The most commonly procedures used are: *forward selection*, *backward elimination* and *stepwise regression*. None of these variable selection procedures is 'best' in any absolute sense. We shall focus on stepwise selection.

Stepwise selection of independent variables is really a combination of backward and forward procedures and is probably the most commonly used method. The first variable considered for entry into the equation is the one with the largest positive or negative correlation with the dependent variable. The F test for the hypothesis that the coefficient of the entered variable is 0 is then

calculated. To determine whether this variable is entered, the F value is compared to an established criterion. One criterion is the minimum value of the F statistic that a variable must achieve in order to enter, called *F-to-enter* (FIN). The other criterion is the probability associated with the F statistic, called *probability F-to-enter* (PIN). If the variable fails to meet entry requirements, the procedure terminates with no independent variables in the equation. If it passes the criterion, the second variable is selected based on the highest partial correlation. If it passes entry criteria, it also enters the equation.

After the first variable is entered, it is examined to see whether it should be removed according to the removal criterion. Two removal criteria may be considered. The first is the minimum F value (FOUT) that a variable must have in order to remain in the equation. Variables with F values less than this *F-to-remove* are eligible to removal. The second criterion is the maximum probability of *F-to-remove* (POUT) a variable can have.

In the next step, variables not in the equation are examined for entry. After each step, variables already in the equation are examined for removal. Vyariables are removed until none remain that meet the removal criterion. To prevent the same variable from being repeatedly entered and removed, PIN must be less than POUT (or FIN greater than FOUT). Variable selection terminates when no more variables meet entry and removal criteria.

3.2 Searching for violations of assumptions

It is don't known in advance whether a regression model is appropriate. Therefore, it is necessary to conduct a search focused on residuals to look for evidence that the necessary assumptions are violated.

3.2.1. Independence of error

Whenever the data are collected and recorded sequentially, you should plot residuals against the sequence variable. Even if time is not considered a variable in the model, it could influence the residuals. If sequence and residual are independent, a discernible pattern should not be seen.

The Durbin-Watson statistic, a test for sequential correlation of adjacent error terms, is defined as

$$D = \frac{\sum_{t=2}^{N} (E_t - E_{t-1})^2}{\sum_{t=1}^{N} E_t^2}.$$

Small values of D indicate positive correlation and large values of D indicate negative correlation. Values of D about 2 indicate absence of correlation.

3.2.2. Linearity and equality of variance

It is convenient to plot the residuals against the predicted values. If the assumptions of linearity and homogeneity of variance are met, there should be no relationship between the predicted and residual values. Residuals can also be plotted against individual independent variables. Again, if the assumptions are met you should see a horizontal band of residuals.

The previously described plots can also be used to check for violations of the equality of variance assumption. If the spread of the residuals increases or decreases with values of the independent variables or with predicted values, you should question the assumption of constant variance of Y for all values of X.

3.2.3. Normality

One of the most important assumptions for a regression model is the normality of all the variables, dependent and independent, and the normality of the residuals (e_i). In advance, several transformations of variables to achieve normality has been conducted (see which are the variables used and their transformations). Once the variables used in the model are normal, we have to look at the residuals.

The distribution of residuals may not appear to be normal for reasons other than actual non-normality: misspecification of the model, nonconstant variance, a small number of residuals actually available for analysis, etc. One line of investigation is to construct a histogram of the residuals.

3.2.4. Looking for influential points

Before interpreting the results of a regression analysis, it is a good idea to find out whether the data contain observations that violate important assumptions. When there are several independent variables, one or more multivariate outliers may distort the analysis. To identify these unusual observations different diagnostic statistics need to be considered. The diagnostics fall roughly into three groups:

(a) *Residual statistics* identify potential outliers in the dependent variable (Y).

(b) *Leverage statistics* identify potential outliers in the independent variables.

(c) *Influence statistics* combine the effects of leverage and residuals to identify influential cases.

Observations having either extreme leverage or large residuals are said to be potentially influential. Influence statistics confirm whether or not the potentially influential cases exert undue force on the regression.

3.2.4.1 Leverage measures

Hatdiag Diagonal elements of the 'hat', or projection, matrix (h_{ii}). The h_{ii} vary between $1/n$ and 1, with an average value of p/n. X is the $(n \times p)$ matrix of centered independent variables; x^t_i is the ith row of X:

$$(1/n) + x_i^t (X^t X)^{-1} x_i .$$

Mahal Mahalanobis distance: the distance of each case to the mean of all cases used in the regression equation. Computed using only the independent variables:

$$(n - 1)\left[h_{ii} - \frac{1}{n}\right].$$

3.2.4.2 Residual measures

Residual The usual residual $e_i = y_i - \hat{y}_i$.

Stresid The standardized residual, $r_i = \dfrac{e_i}{\hat{\sigma}\sqrt{1 - h_{ii}}}$, is the usual residual divided by an estimate of its standard error.

3.2.4.3 Influence measures

Cook Cook's distance is a measure of the influence of the ith case on the estimated regression coefficients:

$$\frac{e_{(i)}{}^2 h_{ii}}{p\,\hat{\sigma}^2}.$$

3.2.5. Measures of co-linearity

Co-linearity refers to the situation in which there is a high multiple correlation when one of the independent variables is regressed on the others. The tolerance of a variable is a commonly used measure of co-linearity. The tolerance (TOL) of variable i is defined as $1 - R^2_i$, where R_i is the multiple correlation coefficient when the ith variable is predicted from the other independent variables. If the tolerance of a variable is small, it is almost a linear combination of the other independent variables.

4. Original and transformed variables used in the models

The original variables considered in this study are: *Partgrao* (Particle concentration for Grao sampling site), *Partherr* (Particle concentration for Herrero sampling site); SO_2grao (SO_2 concentration for Grao sampling site), SO_2her (SO_2 concentration for Herrero sampling site); *Direc* (wind direction), *Tempseco* (air temperature) and *Veloc* (wind speed) as meteorological parameters.

Different tests of normality have been conducted to conclude that the only normal variable is Tempseco.

Following different methods of transformations of variables to achieve normality, the normal transformed variables are:

$$rpargra = \sqrt{Partgrao} \qquad rparher = \sqrt{Partherr} \qquad rSO_2gra = \sqrt{SO_2grao}$$

$$rSO_2her = \sqrt{SO_2\,her} \qquad tddirec = \frac{(Direc)^2 - 1}{2} \qquad \ln tdvel = \ln(2\sqrt{Veloc} + 2\ .$$

Finally, needless to say that the models have been worked out using the transformed variables.

5. Results and discussion

The correlation matrix between the variables is shown in *Table 1*.

Table 1. Correlation matrix

Correlation	tddirec	lntdvel	tempseco	rparher	rpargra	rSO_2her	rSO_2gra
tddirec	1	0.013	– 0.176	0.175	0.336	0.064	0.016
lntdvel		1	0.328	–0.372	–0.285	–0.044	–0.051
tempseco			1	–0.285	–0.336	–0.147	–0.142
rparher				1	0.594	0.263	0.021
rpargra					1	0.185	0.004
rSO_2her						1	0.467
rSO_2gra							1

The low level of linear relationship between the independent or explicative variables can be seen, thus avoiding possible problems of multico-linearity.

Here are the two models of linear regression:

Model 1: Air particle concentration = f (meteorological parameters),
Model 2: Air particle concentration = f (meteorological parameters, SO_2 concentration).

Using the stepwise method, the regression parameters are seen in *Table 2*.

Table 2. Linear regression models

	Linear equation	Multiple R
Model 1	rparher = –0.324 lntdvel + 0.149 tddirec – 0.152 tempseco	0.4353
	rpargra = 0.302 tddirec – 0.22 lntdvel – 0.21 tempseco	0.4846
Model 2	rparher = –0.324 lntdvel + 0.228 rSO_2her + 0.14 tddirec – 0.12 tempseco	0.4902
	rpargra = 0.302 tddirec – 0.22 lntdvel – 0.21 tempseco	0.4846

5.1 Model 1

(a) Model 1.1 (Herrero station)

The results given by Model 1 for Herrero station are presented in *Table 3*.

Table 3. Results for Model 1.1

Model 1.1	Variables entered on step number 1. lntdvel	2. tddirec	3. tempseco
Multiple R	0.372	0.412	0.435
F(Sig. F)	57.398(0.0)	36.372(0.0)	27.678(0.0)
Coefficient B	–2.135(b_1) 9.196(b_0)	–2.148(b_1) 0.003(b_2) 8.492(b_0)	–1.859(b_1) 0.002(b_2) –0.045(b_3) 8.979(b_0)
Coefficient Beta	–0.372(Beta1)	–0.374(Beta1) 0.176(Beta2)	–0.324(Beta1) 0.149(Beta2) –0.152(Beta3)
T(Sig. T)	b_1 –7.576(0.0) b_0 24.027(0.0)	b_1 –7.753(0.0) b_2 3.655(0.0) b_0 20.08(0.0)	b_1 –6.389(0.0) b_2 3.062(0.003) b_3 –2.952(0.004) b_0 19.969(0.0)

The first independent variable, lntdvel, selected is the one which shows the greatest correlation with rparher, explaining 37.2% of the variability of the latter. The correlation is statistically significant (F = 57.398, Sig. F = 0.00). The linear model with this single variable turns out in the following way.

The coefficient B1 = -2.135 is statistically significant, that is, different from zero (T = -7.576, Sig. T = 0.0).

The second variable which enters into the model is tddirec, which together with lntdvel explains 41.2% of the variability of rparher. The multiple model with these two variables is significant (F = 36.37, Sig. F = 0.0) as are the respective beta coefficients. The co-linearity diagnostics indicate the low level of linear dependence between the two independent variables.

Finally, the variable tempseco enters into the model. The linear regression equations, described in Tables 2 and *3*, are significant and the independence requirements.

We may consider the independence of the errors since the Durbin Watson test provides a value of 1.4121. On the other hand, randomness can be seen in the different graphs for the study of linearity and equality of variables which confirms this hypothesis (see *Fig. 2*). The fundamental prerequisite of normality is fulfilled, and is confirmed by both the histogram graph for the residues and the Kolmogorov-Smirnov test (K-S Z = 0.858, 2-tailed P = 0.454), see *Fig. 3*. Different outliers are detected, both by Mahalanobis' distance and Cook's, but none are significant enough to distort the results.

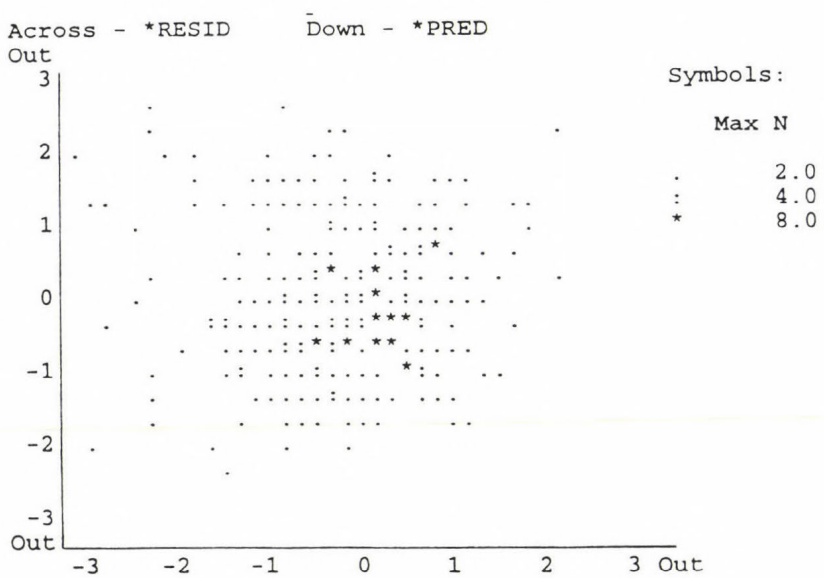

Fig. 2. Model 1.1 Standardized scatterplot.

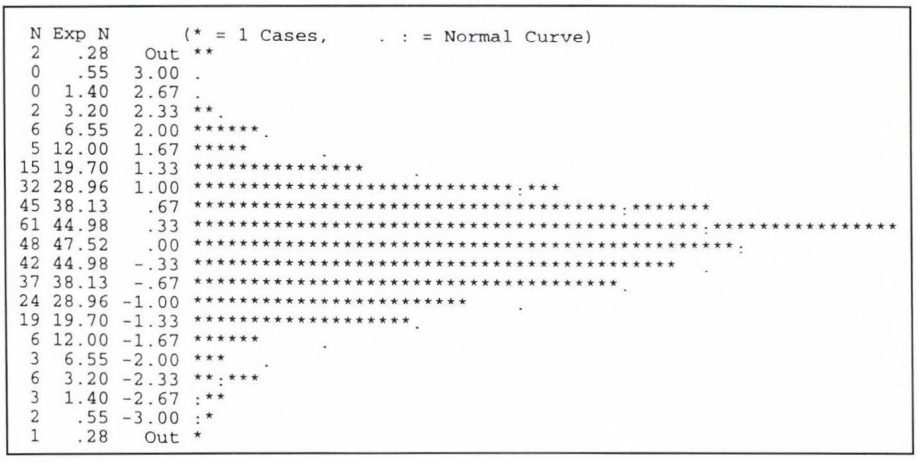

Fig. 3. Model 1.1 Histogram-standardized residual.

(b) Model 1.2 (Grao station)

The results given by Model 1 for Grao station are presented in *Table 4.*

Table 4. Results for Model 1.2

Model 1.2	Variables entered on step number 1. tddirec	2. lntdvel	3. tempseco
Multiple R	0.336	0.443	0.484
F(Sig. F)	45.412(0.0)	43.639(0.0)	36.317(0.0)
Coefficient B	0.004(b_1) 2.946(b_0)	0.004(b_1) −1.363(b_2) 4.734(b_0)	0.004(b_1) −1.036(b_2) −0.051(b_3) 5.286(b_0)
Coefficient Beta	0.336(Beta1)	0.339(Beta1) −0.289(Beta2)	0.3027(Beta1) −0.2204(Beta2) −0.2101(Beta3)
T(Sig. T)	b_1 6.739(0.0) b_0 16.146(0.0)	b_1 7.152(0.0) b_2 −6.104(0.0) b_0 13.8960.0)	b_1 6.38(0.0) b_2 −4.472(0.0) b_3 −4.195(0.0) b_0 14.764(0.0)

In this case the variable which has the greatest correlation with rpargra is tddirec and as such occupies first place by explaining 33.59% of the variability

of the dependent variable. The regression equation is significant (F = 45.41, Sig. F = 0.0) as is the coefficient B1. The next variable which enters into the model, and independently of tddirec, is lntdvel, and this, together with tddirec, explains 44.37%. The regression is once again significant. Last of all comes tempseco to give the full equation for Table 2. All the coefficients are statistically different from zero, producing a significant model for the explanation of rpargra.

There is no serial correlation for the errors (Durbin Watson = 1.382). In the corresponding graphs we can see the existence of linearity in the model as well as the equality of variances. The outliers that are found are not significant and do not influence the significance of the model. Finally, the normality of the residues is supported by the Kolmogorov-Smirnov test (K-S Z = 0.939, 2-tailed P = 0.341) and is shown by the histogram of the residues (*Fig. 4*).

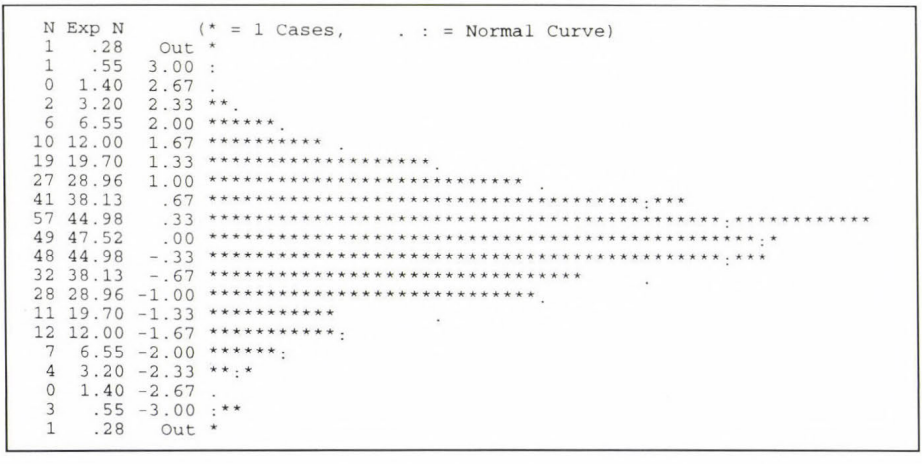

Fig. 4. Model 1.2. Histogram-standardized residual.

(c) Model 1 — Conclusion

Both models are significantly statistical and validated by their residues. The variability explained by independent variables is based on a linear relationship. The rest could be explained by other kinds of non-linear relationships, such as quadratics or cubic relationships. The relationship between air particle concentration and wind direction is direct (positive) while its relationship with wind speed and temperature variables is inverse (negative).

The goodness of fit of Model 1 is expressed by the coincidence between the recorded and expected values in the Normal Probability Plot graph (*Fig. 5*).

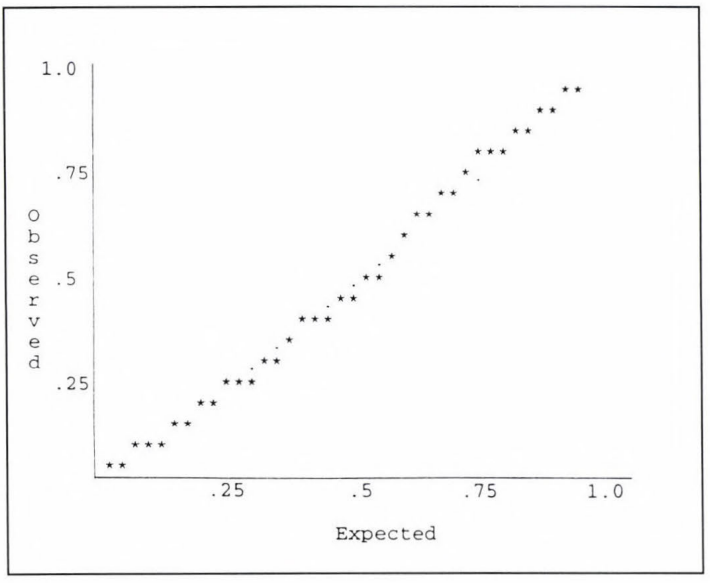

Fig. 5. Model 1.2. Normal probability plot.

5.2 Model 2

(a) Model 2.1 (Herrero station)

In spite of considering the influence of SO_2 in air particle concentrations at Herrero, wind speed remains, as in Model 1, the most important variable for the prediction of rparher. It accounts for 37.21% of the variability of this dependent variable. In second place comes the SO_2 variable, explaining, between the first two variables, 44.99% — more than the three atmospheric parameters explained in Model 1. Afterwards come the temperature and wind direction variables which give the linear equation of Table 2 and a percentage of overall explanation of 49.02%. This equation is significant (F = 27.99, Sig. F = 0.0) and the four explicative variables show a degree of linear independence between each of them (see *Table 5*).

Analysis of the residues shows that this proposed regression model is statistically valid. There is no serial correlation for the residues since the Durbin-Watson test gives a reading of 1.398. Equality of variances and linearity have been achieved. Normality is shown by means of the Kolmogorov-Smirnov test which gives readings of K-S Z = 1.013 and 2-tailed P = 0.256 and is expressed graphically by the histogram (*Fig. 6*). The outliers found are not significant.

Table 5. Results for Model 2.1

Model 2.1	Variables entered on step number			
	1. lntdvel	2. rSO_2her	3. tddirec	4. tempseco
Multiple R	0.372	0.449	0.478	0.49
F(Sig. F)	57.397(0.0)	45.19(0.0)	34.993(0.0)	27.99(0.0)
Coeff. B	−2.135(b_1) 9.1958(b_0)	−2.071(b_1) 0.279(b_2) 7.961(b_0)	−2.085(b_1) 0.267(b_2) 0.002(b_3) 7.371(b_0)	−1.862(b_1) 0.252(b_2) 0.002(b_3) −0.035(b_4) 7.823(b_0)
Coeff. Beta	−0.372(Beta1)	−0.361(Beta1) 0.253(Beta2)	−0.364(Beta1) 0.243(Beta2) 0.161(Beta3)	−0.325(Beta1) 0.228(Beta2) 0.141(Beta3) −0.119(Beta4)
T(Sig. T)	b_1 −7.576(0.0) b_0 24.027(0.0)	b_1 −7.617(0.0) b_2 5.343(0.0) b_0 18.29(0.0)	b_1 −7.786(0.0) b_2 5.19(0.0) b_3 3.442(0.001) b_0 15.961(0.0)	b_1 −6.598(0.0) b_2 4.864(0.0) b_3 2.967(0.003) b_4 −2.37(0.018) b_0 15.75(0.0)

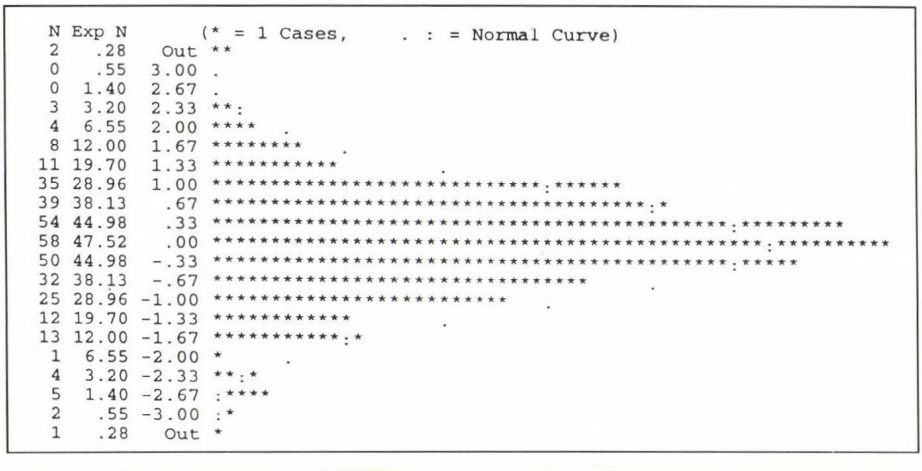

Fig. 6. Model 2.1. Histogram-standardized residual.

(b) Model 2.2 (Grao station)

This model does not require any discussion as it matches exactly with the Model 1.2 described above.

(c) Model 2 – Conclusion

Model 2 is a statistically significant model, in that a substantial part of the variation of the dependent variable can be explained by the independent variables by means of a linear relationship. It is likely that if we introduced some other explicative variable such as atmospheric pressure, we would make a more accurate prediction of air particle concentration.

This model is validated by the residue analysis. Observe that the SO_2 concentration variable is of greater importance when predicting rparher than the meteorological parameters of wind direction and temperature. This, however, is not the case when predicting rpargra — the three meteorological parameters are more influential than SO_2.

The goodness of fit of Model 2 can be studied by observing the Normal Probability Plot graph (*Fig. 7*) in which the ideal case is where the values observed and expected are superimposed on the diagonal line of the rectangle.

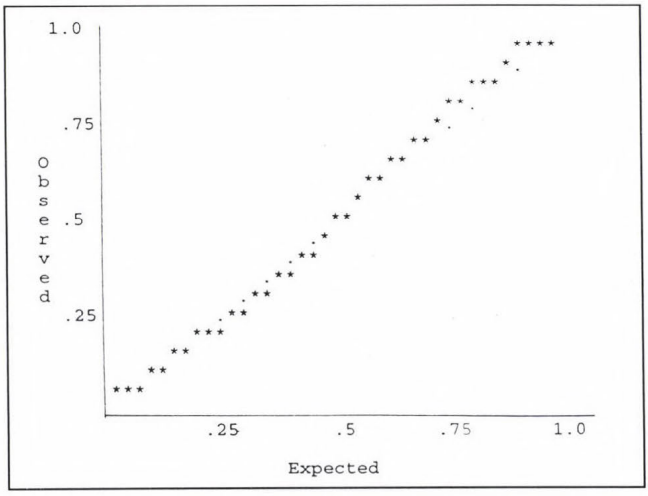

Fig. 7. Model 2.1. Normal probability plot.

5.3. Analysis of bivariate relationships for Grao station

1 [rpargra = f(lntdvel)]

On studying the evolution of air particle concentration in relation to wind speed (*Fig. 8*), it is seen that, at temperatures of below 18°C, there is a slight increase in air particle concentration until the threshold wind speed value of

around 8.2 km/h is reached. At higher speeds air particle concentrations decrease for the whole range of wind directions, but less so for W, NW and N winds.

At temperatures of above 18°C, asymptotic behaviour is seen between air particle concentrations and wind speed, reaching a relationship of independence between the two variables.

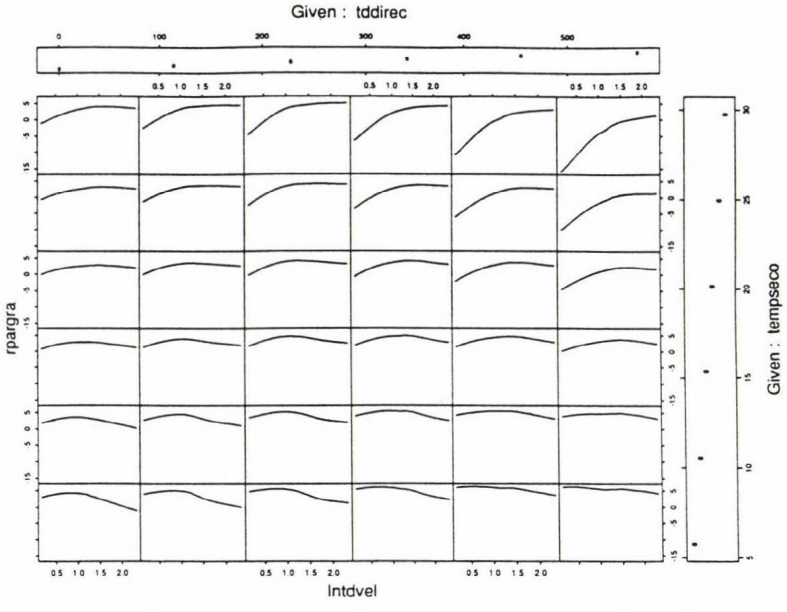

Fig. 8. Multiple linear regression of rpargra compared with lntdvel for tempseco and tddirec values.

2 [rpargra = f(tddirec)]

By studying the variation between air particle concentration and wind direction, we can observe three types of behaviour in relation to temperature, but without appreciable differences in its relationship with wind speed.

At temperatures below 14°C, a slight increase in air particle concentration is noted in the presence of N and NW winds.

In the temperature range of 14–18°C, air particle concentration remains stable, independently of wind direction.

At temperatures above 18°C, a slight decrease in air particle concentration is observed when there is a change from winds of the first quadrant to those of the fourth. This is clearly seen when the evolution of air particle concentration is observed in the light of wind direction. At constant temperatures with wind

speed rising progressively, it can be seen how wind direction becomes less decisive and wind speed gains importance.

3 [rpargra = f(tempseco)]

When we study the influence of temperature on the determination of air particle concentrations with different wind speeds and directions, a marked decrease in air particle temperatures is seen when there is an increase in temperature in the presence of W-NW and NW-N winds.

There is an increase in air particle concentrations as temperature increases when there are N-NE, NE-E and E-SE winds, throughout the whole range of wind speeds.

5.4 Analysis of bivariate relationships for Herrero station

1 [rparher = f(lntdvel)]

At temperatures of above 14°C with N-NW, NW-E, E-SE, SE-S and S-SW winds, a slight increase can be seen (*Fig. 9*) in the air particle concentration until wind speeds of between 6.5 and 10 km/h are reached. At this point, at speeds of over 10 km/h, a marked decrease in air particle concentration begins. At temperatures below 14°C with N-NW, NW-E, E-SE, SE-S and S-SW winds, the trend is similar to the previous case, although the decrease is less marked.

For W-NW and NW-N winds at temperatures of above 14°C, the curve develops two definite inflexion points — the first for wind speeds of 10 km/h and the second for 16 km/h. There is an initial stage (v = 3.24–10 km/h) with a decrease in contamination. At the second stage (v = 10–16 km/h) there is an increase in air particle concentration which later decreases during the third stage (v = 16–26.74 km/h). This same pattern is observed for NW-N winds at temperatures of below 14°C.

2 [rparher = f(tddirec)]

A slight increase in air particle concentration was seen with N-NE, NE-E, E-SE, SE-S and S-SW winds and slight decline with SW-W, W-NW and NW-N. These curves are slightly concave (*Fig. 10*).

At wind speeds below 6 km/h and at temperatures above 18°C, air particle concentrations remain constant in the presence of N-NE, NE-E, E-SE, SE-S and S-SW winds, but increase significantly when winds are SW-W, W-NW and NW-N.

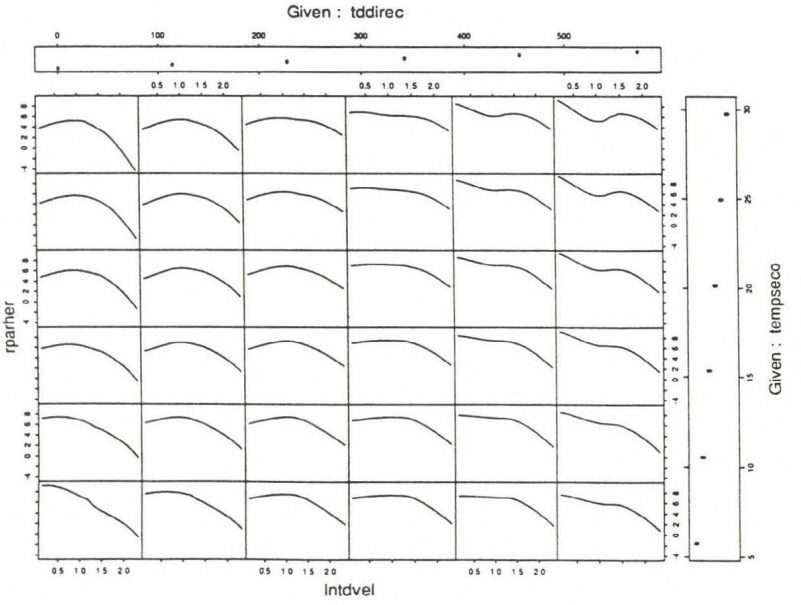

Fig. 9. Multiple linear regression of rparher compared with lntdvel for tempseco and lntdvel values.

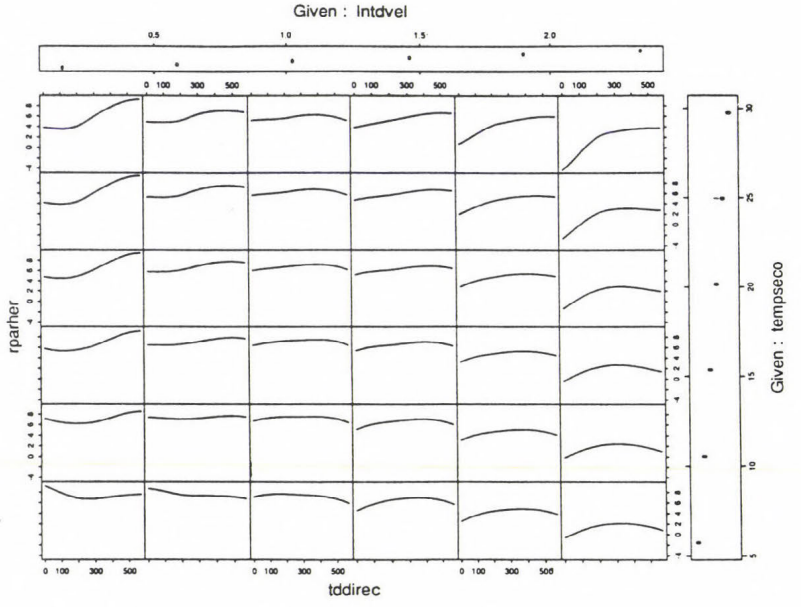

Fig. 10. Multiple linear regression of rparher compared with tddirec for tempseco and lntdvel values.

3 [rparher = f(tempseco)]

Generally speaking, a small decrease in air particle concentrations is noted when temperatures rise. As wind speed increases, we see a progressive decrease in air particle concentrations, also reflected in a lower vertical axis value as temperature rises.

4 [rparher = f(rSO_2her)]

(*a*) *Calm conditions*

The pattern of air particle concentrations with respect to SO_2 concentrations is of a convex nature, and this concavity increases with rises in temperature.

Initially, there is an increase in air particle concentration which rises alongside the increase in SO_2 concentrations until the maximum value for sulphur dioxide is reached. From then on, it starts to decrease (*Fig. 11*).

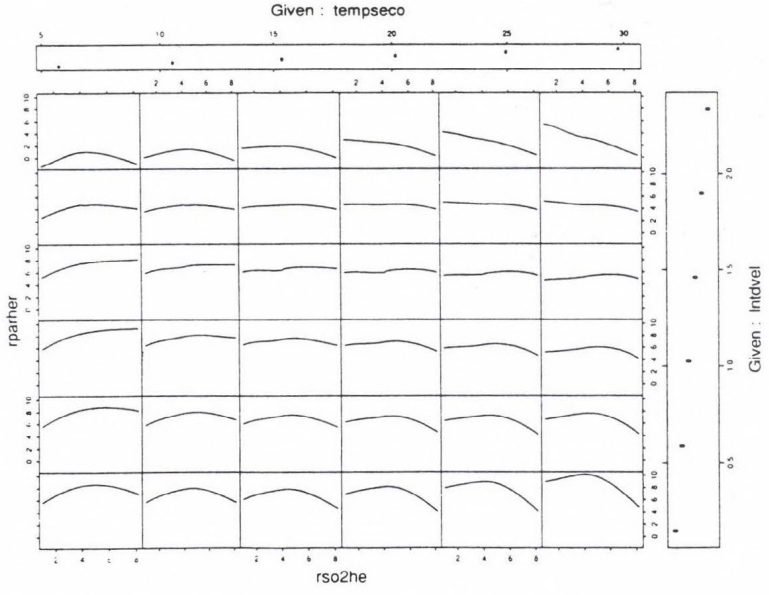

Fig. 11. Multiple linear regression of rparher compared with rSO_2her for Intdvel and tempseco values.

(*b*) *Medium-intensity wind conditions*

Air particle concentrations remain constant at a wide range of temperatures. In the case of T < 10°C, there is an increase in air particle concentrations when the SO_2 is rising, but these remain constant on reaching the maximum value.

(*c*) *Gusts of strong wind*

There is a marked decline in air particle concentrations when the SO_2 values increase.

5 [SO_2her = f(direc)]

SO_2 concentrations reach their maximum values when S, W and NW winds are blowing. Minimum SO_2 values are registered when E and SW winds are blowing. With other wind directions, SO_2 values vary irregularly.

4. Remarks

Model 1

(*a*) *Herrero*

For the proposed multiple regression equation, wind speed is a determining factor in the prediction of air particle concentrations in a linear model. Increases in wind speed are associated with a decline in air particle concentrations in the atmosphere. The atmosphere's ability to disperse pollutants is fundamentally connected to wind speed and to the presence of atmospheric turbulence which helps in their dispersion. Wind is the most important meteorological parameter given its ability to disperse pollutants and to keep air particles in suspension. Other less important climatic factors are temperature and wind direction. With this first model, a clear relationship between wind and the presence of air particles in suspension in the atmosphere was shown experimentally.

(*b*) *Grao*

In the multiple regression equation, it is clearly shown that wind direction is of fundamental importance for the prediction of air particle concentrations in a linear model. The local wind conditions operating in the area can explain the higher or lower levels of air particle concentrations recorded at any time. The remainder of the climatic factors analysed — wind speed and thermal gradient — are of lesser importance at this sampling station.

Model 2

(*a*) *Herrero*

For this model we have proposed a multiple linear regression equation in which we have included the sulphur dioxide concentration measured at this station as

a variable. It has been established that sulphur dioxide concentrations have greater influence in the prediction of air particle concentrations than meteorological parameters such as wind direction and temperature. On the other hand, wind speed remains the most decisive independent variable in the proposed linear model.

The influence of sulphur dioxide on the measurement of air particle concentrations can be explained as a consequence of the presence of secondary or neo-formation air particles which appear in the atmosphere in the form of inorganic components, generally inorganic sulphate salts.

(*b*) *Grao*

The proposed multiple linear regression model establishes that there is no linear dependence between air particle concentrations and sulphur dioxide.

5. Conclusions

The proposed regression models are statistically significant and validated by their residues. As such, they can be taken into account when we predict air particle concentrations linearly. We have only dealt with the linear relationship although a large part of the variations in the dependent variables could be explained using a non-linear relationship. The accuracy of our predictions is affected by the R-square coefficient. Note how the R-square coefficient rises or the variation explained by the model when the new SO_2 variable in Model 2 is considered. This leads us to think of the possibility of considering relevant new variables in order to increase the explained variation and as such, improve the accuracy of our predictions.

The study of wind direction is important for making predictions for the measurement of air particle concentrations at Grao station.

Generally speaking, a decrease in air particle concentrations occurs when temperatures go up, if winds are blowing in the fourth quadrant, and they increase when they blow in the first, second and third quadrants.

In general, we see slight decreases in air particle concentrations when the temperature rises. In conditions of high wind density, SO_2 concentrations are not a determining factor in the prediction of air particle comtamination.

Finally, it is important to remark that those anomalies found in this work may have been caused due to the fact that a unique mathematical model has been used to explain the large variability of meteorological and environmental situations occurring throughout the year.

Acknowledgements—For the final version of this paper we are indebted to the interesting and detailed comments of referees.

References

Anderson, T.W., 1984: *An Introduction to Multivariate Statistical Analysis*. 2nd Edition. Wiley Series, 285-369.

Boix, A., 1992: Estudio la contaminación atmosférica en el área de Castellón y su relación con el regimen de vientos locales. *Tesis de Licenciatura*. Universitat Jaume I., Castellón.

Del Monte, M., 1987: The origin of calcium oxalates on historical buildings monuments and natural out crops. *The Science of the Total Environment 73*, 159-179.

Draper, N.R. and *Smith, H.*, 1981: *Applied Regression Analysis*. 2nd edition. John Wiley and Sons, New York.

Graedel, T.E. and *Mcgill, R.*, 1986: Degradation of materials in the atmosphere. *Env. Sci. Technol, 20,* 1093-1100.

Hallez, S., Goedertier, S. and *Derouane, A.*, 1984: Etude de l'evolution des concentrations en SO2 dans l'air ambiant a Bruxelles de 1968 a 1981. *The Science of the Total Environment 38*, 199-212.

Harrison, R. and *Chirgawi, M.B.*, 1989: The assessment of air and soil as contributors of some trace metals to vegetable plants. II. Translocation of atmospheric and laboratory generated cadmium aerosols and within vegetable plants. *The Science of the Total Environment 83*, 35-45.

Horvath, H., Havenreich, T.A., Kreiner, I. and *Norek, C.*, 1989: Temporal and spatial variations of the Vienna aerosol. *The Science of the Total Environment 83*, 127-159.

Hoskuldsson, A., 1988: PLS regression methods. *Journal Chemometrics 2*, 211-228.

Jaenicke, R., 1984: Physical aspects of the atmospheric aerosol. In *Aerosols and Their Climatic Effects* (eds.: *H.E. Gerber* and *A. Dee*). A. Deepak Publishing Hampton, Va., USA.

Leysen, L., 1989: Air pollution induced chemical decay of a sandy limestone cathedral in Belgium. *The Science of the Total Environment 78*, 263-278.

Lipnick, R.L., 1991: Outliers: Their origin and use in the classification of molecular mechanisms of toxicity. *The Science of the Total Environment 109-110*, 131-153.

Liu, W.K., Tam, J.S.K. and *Wong, M.H.*, 1988: Size dependent citotoxicity as fly ash particles. *Environment International 14,* 473-477.

Matyniak, Z., 1989: Contribution of SO_2 sortion on particulate surface to the air pollution level in the vicinity of coal-fired power plants. *The Science of The Total Environment 83*, 173-179.

Rondia, D. and *Closset, J.*, 1985: Aerosol versus solution composition in occupational exposures. *The Science of the Total Environment 46,* 107-112.

ANNEX

lntdvel	wind speed (km/h)
0.5	4.5
1.0	6.5
1.5	10.0
2.0	16.0
2.5	27.0

tddirec	wind direction (degrees)
0	10
100	135
200	190
300	233
400	270
500	300

rSO_2her	SO_2 concentration ($\mu g/m^3$)
2.0	7.82
4.0	21.00
6.0	40.82
8.0	67.00

rpargra	particle concentration ($\mu g/m^3$)
-15	0.00
-10	6.81
-5	27.20
0	61.30
5	109.00

rparher	particle concentration ($\mu g/m^3$)
-4	0.00
-2	3.02
0	11.90
2	26.62
4	47.19
6	73.61
8	105.88

IDŐJÁRÁS

Quarterly Journal of the Hungarian Meteorological Service
Vol. 100, No. 4, October–December 1996

Influence of terrain configuration on air pollutant concentration

Radmila Cvijović and **Viktor Pocajt**

Faculty of Technology and Metallurgy,
University of Belgrade,
Karnegijeva 4, Belgrade, Yugoslavia

(Manuscript received 15 May 1995; in final form 24 October 1995)

Abstract—This paper is concerned with the evaluation of air pollutant in situ concentration measurement data in Belgrade and the possibility of utilizing information obtained by physical modeling in air pollution prediction and air quality evaluation. The influence of meteorological parameters and objects layout on measurement results is discussed. The results are in accordance with the results of previous investigations, which showed significant influence of control station locations on errors in detecting in situ concentration values. With the advanced technique of physical modeling, it is possible to establish an optimal layout of control stations in air pollution monitoring.

Key-words: air pollution, measurements 'in situ', hydraulic modeling.

1. Introduction

The explanation of the influence of meteorological parameters on the air quality is very significant in solving air pollution problems in cities. If appropriate, scientifically grounded investigations and a well-organized network of control stations are provided, air pollution problem can be successfully analyzed. By using meteorological parameters, it is possible to show their influence on the concentration of pollutants in the atmosphere and to develop methods for prediction of air pollution.

A great number of papers have been presented in which air pollution is correlated to wind direction and velocity and atmosphere stability parameters (*Sonkin et al.*, 1965). It was already pointed out that air pollution diminishes in cities under conditions of increased wind. Maximum of pollutant concentrations was detected in the periods of weak wind and calm conditions. Theoretical and empirical investigations on diffusion from warm sources show

the presence of 'danger', when maximum air pollution is detected in the plume trace. This indicates the relation of the pollutant concentrations with wind direction (*Berlyand*, 1975).

All investigations on the correlation between air pollution in cities and atmospheric stability agree that increased atmospheric stability results in increased air pollution. This conclusion was drawn as a consequence of investigating dominantly low sources. Investigations on atmospheric pollution from high, warm sources lead to the opposite results: in most cases, the pollutant concentrations increase with increasing turbulence and instability. In conditions of low wind velocity, the effect of plume rise is more significant and the site concentration is decreased.

In cities with a larger number of low sources, a significant increase in the air pollution level is detected in the wind velocity range between 1 and 2 m/s. According to measurement data from several cities (*Bezuglaya*, 1986), the average level of air pollution by particles, SO_x and NO_x is increased by 30–140%, compared to levels recorded under conditions of other wind velocities. In the latest investigations, where the average daily SO_x concentrations are correlated with different meteorological parameters, influence of wind has been definitely established and only its significance varies (*Annand* and *Hudson*, 1981).

In monitoring air pollution levels and the influence of human activities on their changes, different reports have been made. These reports and data are bases for the implementation of solutions oriented to decrease atmospheric pollution. Chosen alternatives and solutions, therefore, depend highly on the air pollution reports and data reliability.

2. Investigations and results

This paper is concerned with the evaluation of data, originating from air pollutant in situ concentration measurement data in Belgrade, and the possibility of utilizing the information obtained by physical modeling in air pollution prediction and establishing the optimal control stations layout. Application of modeling enables the investigation and simulation of atmospheric diffusion phenomena under various flow conditions and neutral atmosphere stability (*Cleroux et al.*, 1981; *Alessio et al.*, 1983).

Basic idea was to handle complexity of the air quality determination problem by using the possibilities of hydraulic modeling and to investigate simultaneously and under the same conditions influence of meteorological parameters and terrain configuration on SO_2 concentration.

In situ SO_2 concentration measurements were performed during three months, in winter of 1981, at two locations in Belgrade (the corner of Ivana Milutinovića and Sv. Save streets, and in front of the Main Post building).

Total of 60 air samples was taken by Cassela samplers, and SO_2 concentration was determined by the pararosanilyne method. Test models were made, which were imposed to fluid flow, in regimes analogous to the conditions of mild and moderate wind. In the hydraulic channel (4.5 m long and 0.85 m wide) with recirculation, wind was simulated by water flow and the pollutant was simulated by methylene blue color, released from a point source-stack. The pollutant (i.e. color) concentration was detected indirectly, by measuring color intensity on white adsorbent. Thin sondes, coated with white adsorbent silica gel, were posed at marked places. Adsorption method gives very reliable information on the color concentration above the sonde and, since the diameter of the sonde is only 2 mm, it does not affect fluid flow. The turbulence, which originates from fluid bypassing the objects, is affected only by the terrain configuration and fluid flow, and results in mass transfer, which is analogous to momentum transfer (*Končar-Đurđević*, 1953; *Cvijović*, 1982; *Cvijović* and *Cvijović*, 1992).

The crossroads model

The plume rise above the building is shown in *Fig. 1*; the concentration near to the 'ground' is lower. More intensive wind leads to plume drop and higher pollutant concentrations near the ground and in local turbulence zones.

The pollutant concentration distribution was controlled in situ (*Fig. 2,* measurement units 1 to 4). The dominant wind directions for Belgrade are east-southeast (ESE) and west-northwest (WNW).

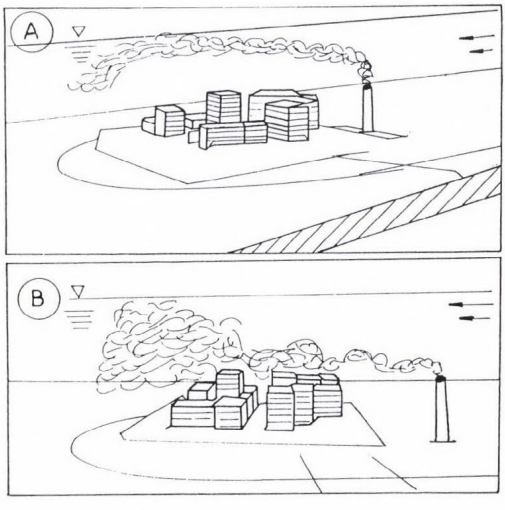

Fig 1. Model with stack in the hydraulic channel.
(*a*) mild wind conditions (Re = 2000); (*b*) moderate wind conditions (Re = 5300).

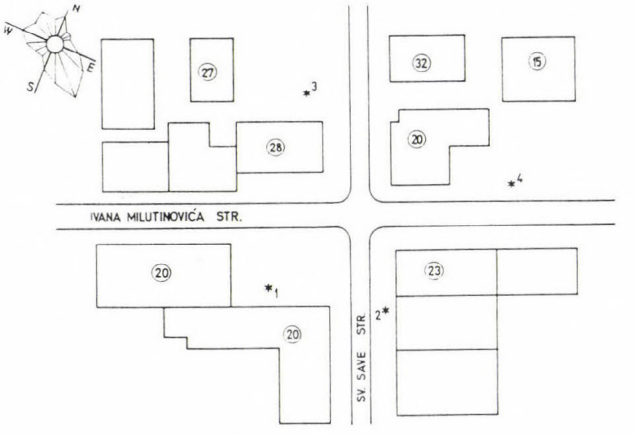

Fig 2. Scheme of the crossroads model, with the measurement units (*) and building height, in meters (numbers in circle). Orientation corresponds to dominant wind directions (ESE and WNW).

The source of the pollutant is the local boiler room stack. Measurement unit 1, managed by the City Health Institute, has been used for air quality control purposes for several years. In order to prove in situ concentration dependence on the meteorological conditions and on the measurement unit position, we posed samplers at the marked places and simultaneously measured SO_2 concentration. Results, in the form of average relative concentration (i.e., the quotient of concentration and average concentration), are shown in *Fig 3.* Histograms are plotted for mild (a) and moderate wind (b) conditions, with parallel model and terrain data.

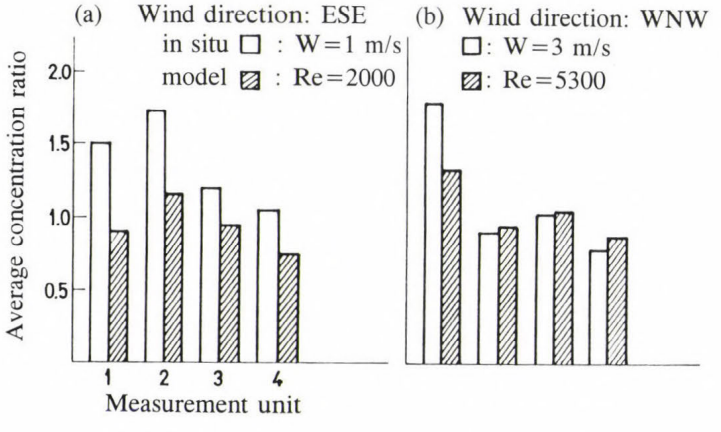

Fig 3. Concentration histogram (corner of Ivana Milutinovića and Sv. Save streets), for mild (*a*) and moderate wind (*b*) conditions.

The agreement of the model results with reality is good, specially for ESE wind direction. Measured pollutant concentration differs for different measurement units. For case (a), measurement unit 1 is the closest to the average concentration (four measurement units), but for case (b) (wind direction WNW) unit 3 is the most representative. It can be concluded that the pollutant distribution on measurement units varies for different wind directions.

For determining the influence of the meteorological parameters on SO_2 concentration, relations between the concentrations for the same wind velocity but different directions were calculated on the basis of model data. In that conditions, concentrations differ by a factor of 1.36.

The influence of the wind velocity was estimated in the same manner, by using model data for the same wind direction but different velocities. Concentration ratio varies by up to 1.26 times.

The influence of the measurement unit position was estimated using the maximum and minimum pollutant concentration ratio. For in situ measurements and ESE wind, the ratio is 1.6; for model measurement and the same wind, the ratio is 1.62.

It can be concluded that for a 'canyon' crossroads wind direction and velocity have similar significance, but the unit position on the measured pollutant concentration is the most significant parameter.

The Main Post model

This model is different from the previous one, since there is no street 'canyon'. In the wind direction (ESE), there is a wide area in the front of the House of Parliament and the park. The pollutant distribution was measured with three units in December, 1979 and January, 1980. The SO_2 source is the local boiling room stack on the Main Post building. The model, which reproduces terrain situation and measurement units layout is shown in *Fig. 4*.

The average concentration ratio (ratio of measured concentrations and average concentration) for ESE wind is shown in the histogram (*Fig. 5*). It can be noticed that with increasing distance from the source, the pollutant concentration decreases. In situ and model measurements are in good accordance for moderate velocity wind from the same direction. High concentration was detected by measurement unit 1, in the 'building shadow' zone, which provides conditions for concentrating the pollutant.

Interesting in situ measurement results were obtained for high wind velocity (up to 13,6 m/s). The concentration measured by unit 1 was slightly decreased, but by units 2 and 3 was increased. This is probably caused by the plume dropping effect - higher wind velocity increases SO_2 concentration. Unfortunately, model measurements for conditions of very strong wind were not performed, due to limited possibilities of flow regulation in the hydraulic channel.

The influence of the wind velocity, described by the ratio of maximal to minimal in situ concentration is significant: the ratio difference is 1.58 times.

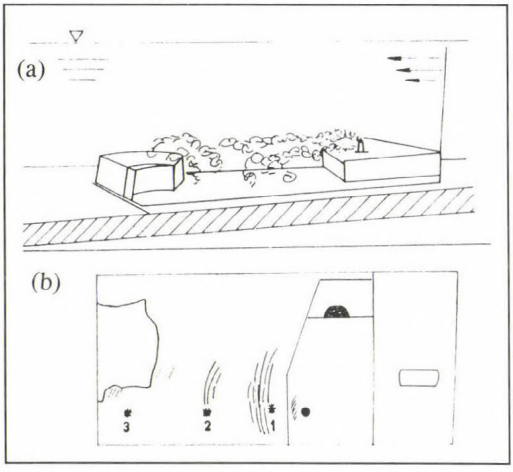

Fig. 4. Model in the hydraulic channel. (*a*) moderate wind velocity (Re = 5300); (*b*) model with measurement units layout.

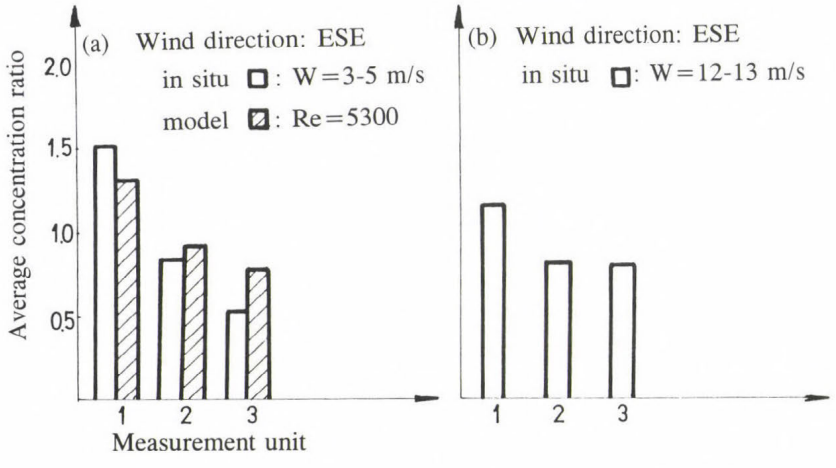

Fig 5. Concentration histogram, location: in front of the Main Post. (*a*) moderate wind; (*b*) strong wind.

The influence of the measurement unit position, which is described by the ratio of maximal to minimal in situ concentration, is very significant: for conditions of moderate wind the ratio differs 2.7 times and for strong wind the

difference is 1.54 times. According to model measurements, predicted difference is 1.54 times.

On the basis of these results, it can be concluded that physical modeling provides a satisfactory degree of analogy of momentum and mass transport phenomena, which are cause of the distribution of pollutant in nature. Influence of objects layout and local turbulence on the concentration was also confirmed.

3. Conclusions

Model measurements exhibit very good accordance with in situ measurements; they are relatively simple, velocity and direction of the wind can be easily changed and objects' layout corresponds to the real situation.

Our investigations have shown that under the conditions of moderate wind velocity (1 to 5 m/s) significance of wind velocity and wind direction are approximately equal. For the model with a street 'canyon' measured concentrations for different velocities (other conditions were same) varied by up to 1.26 times; measured concentration for different wind directions varied by up to 1.36 times. For measurements without a street 'canyon' (Main Post building) and moderate wind velocity, the results varied by up to 1.58 times.

In the analysis of the influence of the measurement unit position, for small and moderate wind velocities, it was found that concentrations varied by up to 1.6 times. Therefore, the influence of the measurement unit position on measured pollutant concentrations is as important as the influence of meteorological parameters.

These investigations can give useful information for establishing a rational and functional network of representative measurement units in the complex structure of cities.

References

Alessio, S., Briatore, L., Elisei, G. and *Longetto, A.*, 1983: A laboratory model of wake-affected stacks emissions. *Atmospheric Environment 17*, 1139-1143.

Annand, W.Y. and *Hudson, A.M.*, 1981: Meteorological effects on smoke and sulfur dioxide concentrations in the Manchester area. *Atmospheric Environment 15*, 799-806.

Berlyand, M.E., 1975: *Contemporary problems of atmospheric diffusion and atmospheric pollution* (in Russian). Gidrometeoizdat, Leningrad.

Bezuglaya, E., 1986: *Atmospheric air-pollution monitoring* (in Russian). Gidrometeoizdat, Leningrad.

Cleroux, R., Roy, R. and *Robert, A.*, 1981: Relationships between sulfur dioxide pollution and meteorological factors in Montreal. *J. Environ. Syst. 10*, 165-181.

Cvijović, R.S., 1982: *Application of Adsorption Method and Hydraulic Analogy in Pollutant Distribution Modeling* (in Serbian). *Ph. D. Thesis*, University of Belgrade, Belgrade.

Cvijović, R.S. and *Cvijović, S.D.*, 1992: Some characteristic hydraulic models of pollutant transfer. *J. Serb. Chem. Soc. 57 (5-6)*, 375-384.

Končar-Đurđević, S., 1953: Application of a new adsorption method in fluid flow. *Nature 172*, 858.

Sonkin, L.R. and *Hrapachenko, V.*, 1965: Dependence of pollution in cities on meteorological conditions in summer season (in Russsian). *Trudy, G.G.O.*, No. 293, 68-77.

IDŐJÁRÁS

Quarterly Journal of the Hungarian Meteorological Service
Vol. 100, No. 4, October–December 1996

The effect of Belgrade on urban precipitation

Miroslava Unkašević

Institute of Meteorology, University of Belgrade,
11001 Belgrade, Dobračina 16, Yugoslavia

(Manuscript received 6 June 1995; in final form 27 December 1995)

Abstract—In this study daily, monthly, seasonal and yearly precipitation in the Belgrade area network during the period 1951–1985 are analyzed. Daily precipitation amounts were expressed in millimeters, which included the melted water equivalent for snow. Averaged annual minimum precipitation which refers to the spatial pattern is recorded northeasterly and maximum precipitation southwesterly from Belgrade confirming that the direction southwest-northeast is the direction of decreasing of station elevations.

It is shown that the average annual increase of precipitation on urban stations is about 11% in comparison with rural stations. This indicates that some individual rain intensity centres of showers or thunderstorms that develop or pass over Belgrade industrial area appear to be significant (*Ćurić* and *Janc*, 1987).

However, monthly precipitation in the Belgrade urban area does not seem to follow the rule that urban precipitation is always higher than rural, since contrary results have been found during the analyzed period.

The examined frequency distributions of mean daily temperature and distributions of total precipitation amounts as a function of mean daily temperature for Belgrade-Observatory for January and October (1951–1985) show that most of precipitations are observed below the median of daily temperatures.

Key-words: precipitation, urban effect, Belgrade area network.

1. Introduction

In a review of urban effects on precipitation in the United States, *Changnon* (1969) stated that if topographic effects are eliminated, urban produced increases in annual precipitation have been found to be from 5–8%. In the mid-western cities of Chicago, Champaign-Urban and Tulsa, warmer half-year precipitation totals were 4–6% higher in urban than rural areas; while for the colder half-year, the values were 6–11%. *Thomas* (1971) reports that in Toronto (Canada), with 35 precipitation observing stations, many in operation for 10–15 years, no urban effect on precipitation has been discovered. *Huff* and *Changnon*

(1972) report that for St. Louis, urban effects caused an increase in precipitation in and downwind of the city in all seasons, and that the average summer rainfall was increased by 6–15% for distances up to 40 km downwind of the city. The controversial results in La Porte data (*Changnon*, 1969) with differences reported as 30–35% for warm and cold season precipitation, perhaps should be considered a special case. Although the urban area or microscale precipitation pattern did not appear to differ on an annual basis from the regional precipitation pattern, *Sanderson et al.* (1973) concluded that, on a seasonal basis, Detroit received less precipitation than the surrounding rural areas in autumn and winter and about 20% more in summer.

Oke (1984) suggests that the greater frequency of rain initiation over urban and industrial areas is tied to three urban-related factors:

(1) thermodynamic effects which lead to more clouds, higher cloud bases and greater cloud instability,
(2) mechanical and thermodynamic effects that produce confluence zones where clouds and rain initiate,
(3) the enhancement of the cloud droplet coalescence process due to the addition of giant nuclei.

These factors appear to combine to initiate more cloud cells over urban-industrial regions in summer which, increase the probability of cell merger and the probability of heavier rain.

2. Precipitation in Belgrade area network

It is evident that there is an important gap in basic knowledge concerning small-scale rainfall processes which is important for design and analysis of urban precipitation and runoff (*Allerup*, 1991). There is an urgent need for coupling meteorology, hydrology and statistics in order to make improvements in urban precipitation characterization. The lack of densely spaced precipitation stations with good historical records, inadequate instruments for air-borne measurements of the effects on precipitation systems, and difficulties associated with delineating orographic, maritime, and gage-exposure effects are the primary reasons for insufficient research.

However, the recent development of air-borne nuclei measuring instruments has led to selected measurements of condensation and freezing nuclei over several urban areas. These facts give evidence that urban-induced nuclei concentration is high and probably sufficient to produce the observed changes in precipitation, whereas other studies (*Chandler*, 1976; *Landsberg*, 1981; *Goldreich*, 1985; *Oke,* 1986) have indirectly shown the importance of the urban thermal effects.

In this Section daily, monthly, seasonal and yearly precipitation in Belgrade area network during the period 1951–1985 are analyzed because in this period most of precipitation stations were in operation (48). The stations in the major

area of Belgrade used in this work are shown in *Fig. 1*. The area, with its particularities (changes in height from 70 m (Boljevci) to 310 m (Avala)) presents characteristics making it particularly interesting for such studies. The Belgrade basin covers approximately 560 km^2 area with the hill of Avala to the south and two great rivers (Sava and Danube) and lowlands to the east, north and west. The precipitation stations taken into account (*Table 1*) are representative of the different areas present in this district: rural, suburban and urban territories. The Meteorological Station of the National Observatory of Belgrade which is situated at 132 m above mean sea level is the basic station.

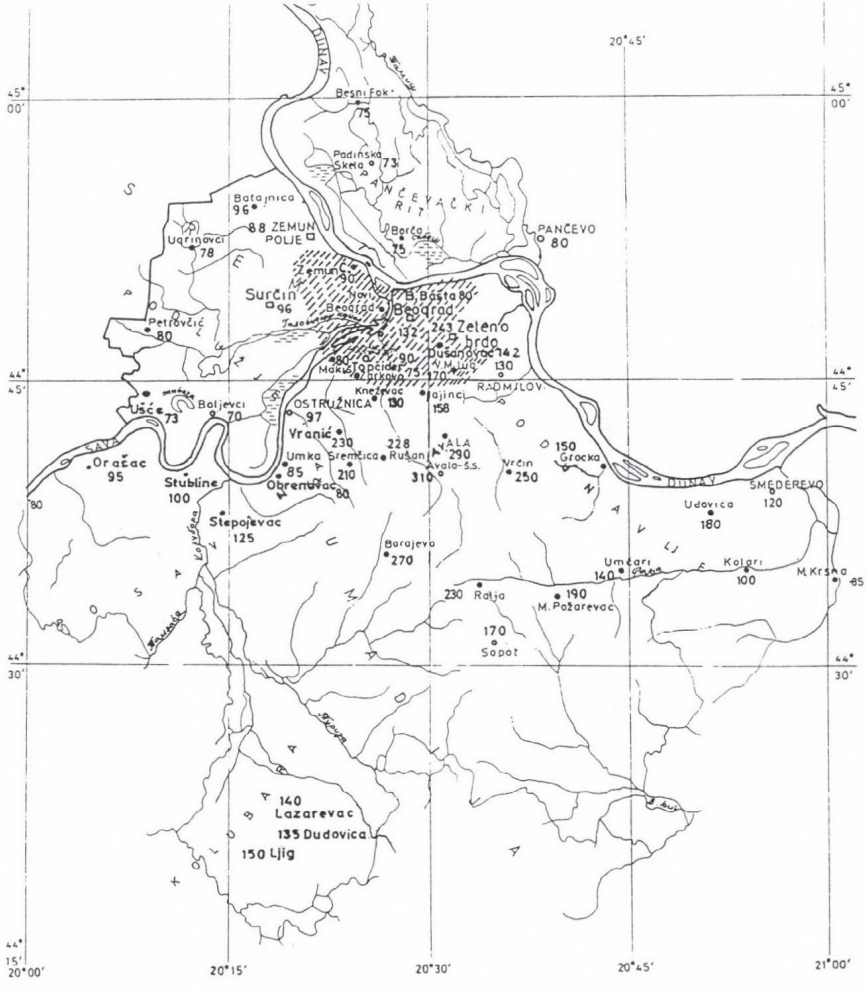

Fig. 1. Map of Belgrade precipitation network. The shaded area represents the Belgrade urban area. The numbers are related to the station altitude (m).

Table 1. Averaged monthly and annual precipitation (mm) during the period 1951–1985 in the Belgrade area

			MONTH												
No	Station	H(m)	Jan	Feb	Mar	Apr	May	June	July	Aug	Sep	Oct	Nov	Dec	Σ
1	Avala - Šum. upr.	290	52.4	48.7	51.7	60.0	76.7	90.8	71.2	60.4	57.2	47.5	59.1	62.8	738.3
2	Avala - Šuplja st.	310	48.5	46.0	46.6	56.5	74.9	87.7	69.0	53.7	54.9	45.8	56.5	59.3	699.4
3	Batajnica	96	43.7	41.2	41.2	46.2	60.2	92.9	62.3	52.1	45.9	41.3	52.1	58.5	637.6
4	Barajevo	270	59.3	43.3	45.0	54.7	81.6	92.3	67.5	64.2	51.6	51.6	52.6	61.8	719.1
5	Beograd (Obs)	132	49.1	46.4	46.5	55.9	72.2	95.6	70.4	53.9	53.1	42.5	55.7	58.7	700.2
6	Besni Fok	75	39.0	41.1	36.8	44.1	57.3	82.1	63.8	46.4	44.0	39.3	49.1	51.6	594.5
7	Botanička Bašta	80	48.6	47.1	46.3	57.4	73.9	95.8	71.8	54.7	52.0	42.8	58.1	62.3	710.7
8	Borča	75	47.2	44.1	42.2	52.4	64.3	93.3	63.5	51.8	47.2	41.4	53.1	57.9	658.4
9	Boljevci	70	46.1	46.1	42.3	50.9	68.5	89.7	63.1	59.1	51.4	45.0	54.4	59.7	672.3
10	Veliki Mokri Lug	160	56.0	50.5	51.6	59.7	74.2	102.4	75.7	52.7	54.7	45.8	57.8	62.7	743.6
11	Vranić	230	53.0	48.8	50.1	60.3	79.5	93.5	73.8	64.5	56.0	48.1	61.1	65.7	754.4
12	Vrčin	250	53.3	49.0	50.2	59.8	74.7	92.3	71.2	51.2	53.4	45.2	58.7	60.3	719.3
13	Grocka	250	41.7	40.0	40.8	52.3	66.3	76.1	60.0	47.5	43.7	43.0	52.5	50.3	614.2
14	Dudovica	135	57.3	53.6	59.2	67.8	95.7	97.0	82.0	72.0	60.1	54.2	67.4	67.8	834.0
15	Dušanovac	142	52.8	47.0	48.5	57.5	72.7	95.7	69.4	53.9	50.2	43.1	55.9	62.6	709.2
16	Žarkovo	75	48.5	44.8	43.5	53.4	70.2	87.7	64.4	51.1	50.3	44.5	54.3	58.5	671.3
17	Zeleno brdo	243	44.4	41.6	45.0	54.0	75.8	97.3	75.1	50.6	51.3	44.8	54.4	57.7	692.0
18	Zemun Čukovac	90	49.0	45.0	44.8	54.8	68.9	91.9	68.1	53.8	53.1	43.6	54.3	59.5	686.7
19	Zemun Polje	88	39.4	39.6	37.7	49.4	67.7	85.3	67.9	50.8	45.5	42.9	50.5	52.9	629.6
20	Jajinci	158	47.5	44.3	44.9	57.5	74.4	97.7	71.7	54.2	52.3	43.2	55.0	58.1	692.6
21	Kneževac	130	49.7	45.6	46.9	57.9	71.9	94.1	71.0	59.1	53.9	44.8	55.5	60.1	710.5
22	Kolari	100	49.8	48.5	43.9	57.1	68.3	76.7	62.6	53.1	46.8	43.9	54.5	56.4	661.6
23	Lazarevac	140	59.8	55.0	60.8	63.7	85.1	99.3	76.8	69.2	56.3	49.8	64.1	68.4	799.8
24	Ljig	150	58.1	59.5	59.4	72.0	91.7	99.5	85.6	73.5	59.0	55.1	63.3	73.1	856.8
25	Makiš	80	47.4	42.5	42.2	50.7	70.2	86.9	61.9	56.3	49.4	42.1	50.5	57.4	640.5
26	Mala Krsna	85	46.2	40.9	43.0	53.9	73.0	85.5	65.9	51.5	45.1	42.5	53.8	55.1	655.8
27	Mali Požarevac	190	42.1	36.5	40.7	52.4	68.1	79.7	60.0	56.0	49.3	42.5	50.6	52.2	631.1
28	Obrenovac	80	45.8	41.8	43.5	52.8	65.5	89.4	67.4	62.8	52.6	46.7	53.0	57.3	678.6
29	Orašac	95	47.8	45.4	47.5	56.5	62.5	95.8	63.1	59.5	52.2	45.4	55.9	55.7	690.3
30	Ostružnica	97	49.6	44.1	44.3	51.5	71.8	85.7	63.6	57.8	50.5	44.1	54.2	59.2	676.3
31	Pančevo	80	40.8	40.2	40.7	52.2	71.5	90.7	63.5	52.5	43.7	40.0	55.1	56.0	647.0
32	Padinska skela	73	38.0	40.6	38.6	48.5	60.2	81.0	67.4	50.0	43.3	40.9	52.5	52.2	613.0
33	Petrovčić	80	47.2	46.2	44.5	52.6	65.8	88.6	62.3	58.2	50.7	45.4	53.3	61.8	676.6
34	Radmilovac	130	46.4	42.9	42.5	56.0	71.8	85.7	71.5	50.1	47.3	43.7	54.9	55.8	668.4
35	Ralja	230	50.3	43.4	47.5	58.0	73.0	90.7	70.7	55.1	52.9	49.1	55.3	59.9	706.1
36	Rušanj	228	52.8	47.5	46.9	58.5	72.5	93.1	63.9	64.5	57.3	46.5	57.1	61.2	721.9
37	Smederevo	120	46.7	43.0	43.1	55.5	71.2	88.0	62.7	51.5	49.1	44.5	55.2	53.5	664.0
38	Sopot	170	52.6	50.2	50.4	59.9	74.0	88.7	63.6	59.0	51.4	44.9	55.2	60.3	710.2
39	Sremčica	210	53.4	46.1	47.8	60.0	78.6	97.1	77.1	63.1	52.8	51.0	58.9	65.8	751.7
40	Stubline	100	46.6	48.7	51.5	58.4	71.4	91.8	74.0	58.4	54.8	50.6	59.3	56.4	721.9
41	Stepojevac	125	51.4	46.6	46.7	55.1	76.6	87.7	71.3	56.0	50.5	50.2	59.1	59.2	710.4
42	Surčin (Airport)	96	45.9	43.5	42.5	49.9	68.2	88.9	63.4	58.6	51.9	41.4	52.5	56.2	662.9
43	Topčider	90	55.3	47.7	49.8	57.1	75.7	93.3	76.4	58.0	53.0	43.2	57.1	60.8	727.5
44	Ugrinovci	80	41.5	41.5	36.7	43.8	59.8	81.2	60.8	56.2	46.4	44.3	51.2	55.5	618.7
45	Udovice	180	48.3	47.1	47.2	64.0	83.1	96.1	65.0	55.3	53.3	46.7	60.9	60.3	727.4
46	Umka	85	49.0	43.2	44.7	56.7	72.2	91.3	66.8	59.2	51.4	47.2	56.7	59.4	697.7
47	Umčari	140	46.6	45.5	46.0	55.8	66.7	77.9	62.4	53.0	44.1	44.2	50.3	58.7	651.2
48	Ušće	73	48.1	46.0	49.7	55.3	64.5	85.7	65.9	58.1	52.5	49.8	58.7	60.6	695.0

The numbers: 5, 7, 10, 15, 16, 18 are related to urban, 3, 4, 8, 17, 23, 24, 25, 26, 27, 28, 29, 31, 32, 37, 38, 39, 42, 43, 46, 48, to suburban and 1, 2, 6, 9, 11, 12, 13, 14, 19, 20, 21, 22, 30, 33, 34, 35, 36, 40, 41, 44, 45, 47, to rural stations. The station altitude (m) is given on the right-hand side of the station name.

Table 1 shows the annual and monthly data patterns for precipitation, as recorded in the different stations. Changes in annual precipitation are less than changes in monthly precipitation. Maximum changes occur in May, June and October and minimum in January. It may be concluded that greatest changes in warm season are caused by different thunderstorm precipitation. Annual precipitation in the Belgrade network area depends on the elevation of stations. Regional patterns of annual and seasonal precipitation are shown in *Fig. 2.*

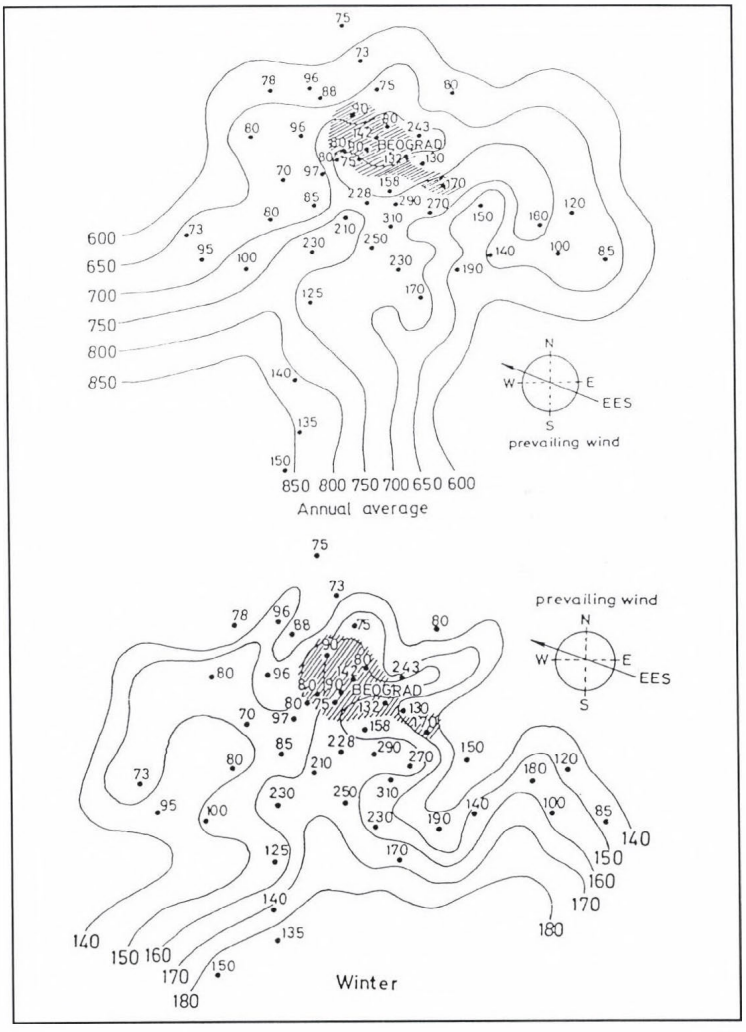

Fig. 2. Annual and seasonal precipitation patterns (mm), during the period 1951–1985 in the Belgrade area. The shaded area represents the Belgrade urban area. The numbers are related to station altitude (m).

Continued Fig. 2.

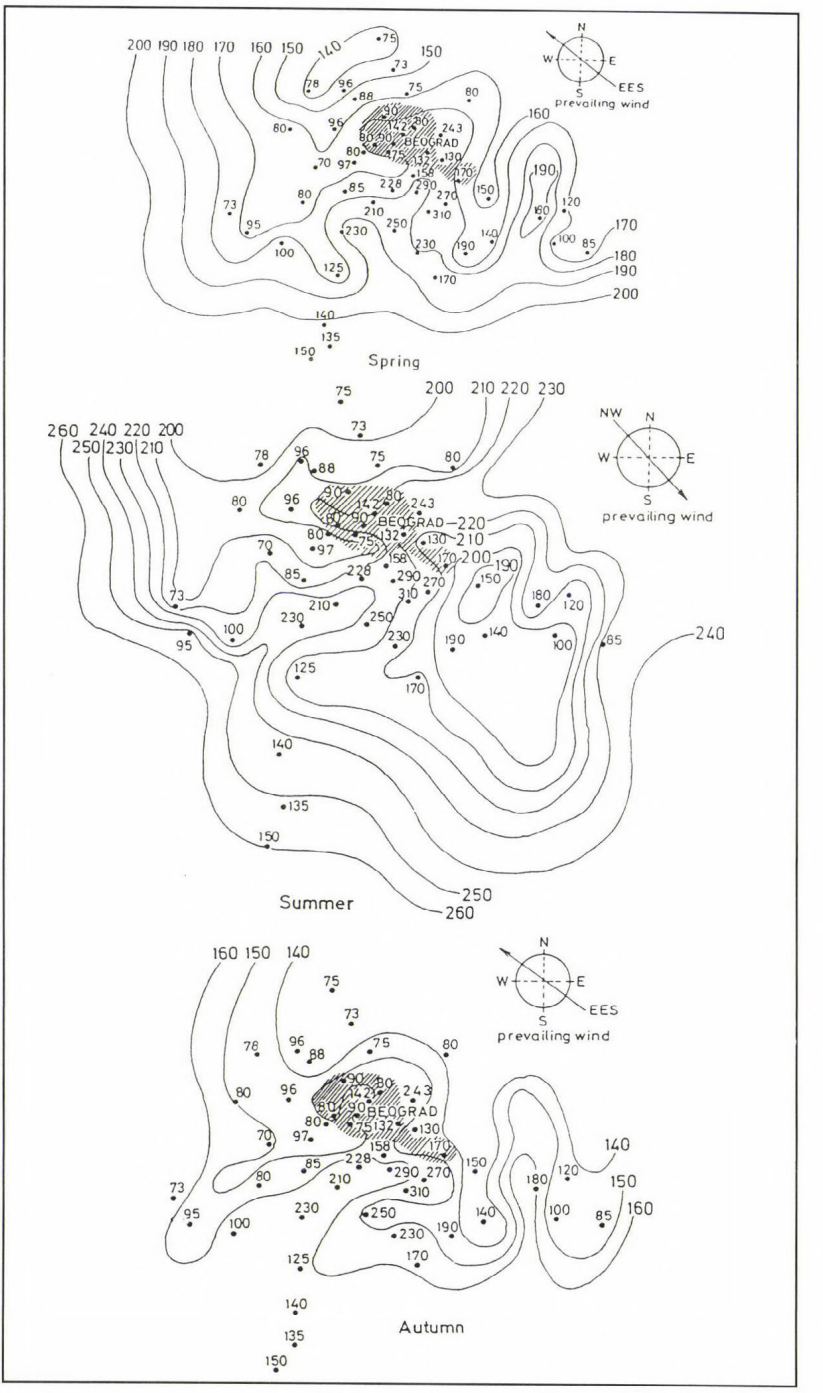

Averaged annual minimum precipitation amounts are recorded to the northwest from Belgrade in the area between precipitation stations Besni Fok and Zemun, i.e. in the area with the lowest elevations of the stations. Higher values over these precipitation amounts are recorded on stations Batajnica, Ugrinovci, Petrovčić Surčin, Pančevo and on stations along Danube river towards to the station Smederevo. Precipitation stations along Sava river and at the western border of Belgrade area have more of annual average precipitation by 20 to 50 mm than those stations on the eastern border of Belgrade area. This could be caused by updraft and cooling air on the west side of the Belgrade area which gave less precipitation than the east side of the Belgrade area.

However, the greatest precipitation amounts are registered in the region of Lazarevac towards Ljig, confirming that the direction southwest-northeast is the direction of decreasing in the station elevations.

The seasonal precipitation distribution (Fig. 2) shows that during spring and summer the relatively high amounts of precipitation are recorded in central parts of Belgrade city. In spring, the minimum precipitation amounts are recorded at the stations Besni Fok (138 mm) and Ugrinovci (140 mm), increasing to the south. The similar space distribution of precipitation is observed during summer but with greater amounts towards the prevailing wind. The precipitation amount decreases in the cold part of the year in all stations (Fig. 2). So in autumn and winter the amounts between 150 and 160 mm are registered in the Belgrade area (Fig. 2) giving evidence to more uniform distribution in the cold part of the year.

3. The effect of urban heat island on urban precipitation

First, we used the Student's t-test (*Brazel* and *Balling*, 1986) to determine differences in the means in periods 1888 to 1969 and 1970 to 1991 (period of great urbanization) in Belgrade-Observatory.

This statistic is determined as

$$t = \frac{(\overline{P}_2 - \overline{P}_1)}{\left(\left[\left(N_1 S_1^2 + N_2 S_2^2\right)/\left(N_1 + N_2 - 2\right)\right]\left[1/N_1 + 1/N_2\right]\right)^{1/2}},$$

where $(\bar{P}_2 - \bar{P}_1)$ represents the difference in group means, N_1 and N_2 are the number of cases within each subsample, and S_1 and S_2 are the standard deviations in the subsamples. When t is outside the bounds of the two-tailed probability of the Gaussian distribution tg (equal to 1.96 at the 0.95 confidence level), a significant shift in the means is assumed. The results are represented in *Table 2*.

The Student's test indicates that October have been characterized by slight decrease and January and February by slight increase in precipitation, so that there are significant changes in precipitation in the urban area during the period of examination.

Table 2. Precipitation time series descriptive statistic during the period 1888–1991 for Belgrade-Observatory

	Jan	Feb	Mar	Apr	May	Jun	Jul	Aug	Sep	Oct	Nov	Dec
t	1.99	2.03	0.49	-0.30	-0.06	1.64	0.92	-0.09	1.24	-2.13	0.33	1.79
tg	1.96	1.96	1.96	1.96	1.96	1.96	1.96	1.96	1.96	1.96	1.96	1.96

The 1951–85 frequency distributions of mean daily air temperature for Belgrade Observatory for January and October are shown in *Fig. 3* (*Isaac* and *Stuart*, 1992). Superimposed on Fig. 3 are the distributions of total precipitation amount as a function of mean daily temperature. The mean daily temperature was obtained by averaging the daily maximum and minimum temperatures. As it is evident from these graphs, most of the precipitation in October is observed at temperatures below the median of daily temperatures (65.6% represented by the hatched area on Fig. 3). This fraction of the total monthly precipitation for January is 46.9%. This shows that average daily temperatures can be used to identify other temperature-dependent phenomena as freezing rain or fog which is significant for urban climate.

In order to determine the effect of the urban heat island relative to the surrounding areas on urban precipitation, a spatial-temporal section was used with the mean values of the minimum temperatures collected at stations located on the line from station Zemun Polje to station Radmilovac. The section gives month by month trends of the minimum temperature from the rural station Zemun Polje through the city up to the rural station at Radmilovac during the period 1970–1989 and is represented in *Fig. 4* (*Unkašević*, 1991).

Taking into consideration these minimum temperatures, the presence of the heat island appears clearly either during the winter months or during the summer months, it increases from winter to summer.

ΔT_{S-S} and ΔT_{u-S} in *Table 3* concern the temperature differences between two suburban stations Padinska Skela and Pančevo (with elevation difference of 7 m) as well as the urban station Dušanovac and suburban station Surčin (Airport) (with elevation difference of 46 m). The terms ΔT_{S-r} and ΔT_{u-r} refers to the temperature differences between suburban and rural station located in Zeleno Brdo and Radmilovac (with elevation difference of 113 m), and urban station Beograd (Observatory) and rural station Ostružnica (with elevation difference of 35 m).

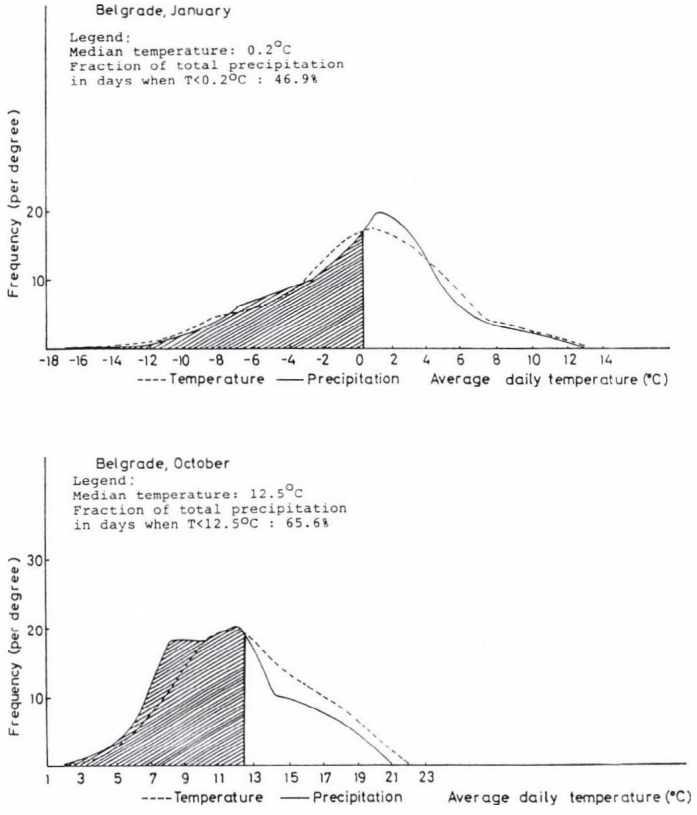

Fig. 3. Frequency distribution of temperature and total precipitation during January and October at Belgrade-Observatory during the period 1888–1991.

In a general sense, it is obvious that the city generates the heat island with temperatures increasing from suburbs to the center. Due to topographic (changes in elevation) and other complicating factors it is hard to place a definite value on the magnitude of the heat island, but it seems reasonable to suggest a figure of at least 2–3°C (*Unkašević*, 1991).

Research on the effect of the urban area on precipitation patterns has been done by a comparison of seasonal precipitation patterns for adjacent urban-rural pairs of stations of similar heights. The results, being represented in *Table 4*, show that maximum differences are obtained in four pairs of stations during spring and summer (rainy season) and in two pairs of stations during winter (Veliki Mokri Lug – Jajinci and Zemun Ćukovac – Zemun Polje). These maximum differences are registered downwind of the city in all seasons.

In the Belgrade area, warmer half-year precipitation totals were 3.4–37.4 mm higher in urban than in rural areas; while for the colder half-year, the differences were 4.9–30.6 mm. In the average value, for all pairs of stations,

the rate of precipitation change has minimum in autumn (11.5 mm) and maximum in winter (20.4 mm). Namely, it is obvious that the average annual increase in precipitation of urban stations is about 11% in comparison with adjacent rural stations of similar heights, i.e. maximum annual increase was registered on urban station located in strong industrial zone of the Belgrade area (stations: Botanička Bašta, Dušanovac and Zemun Ćukovac).

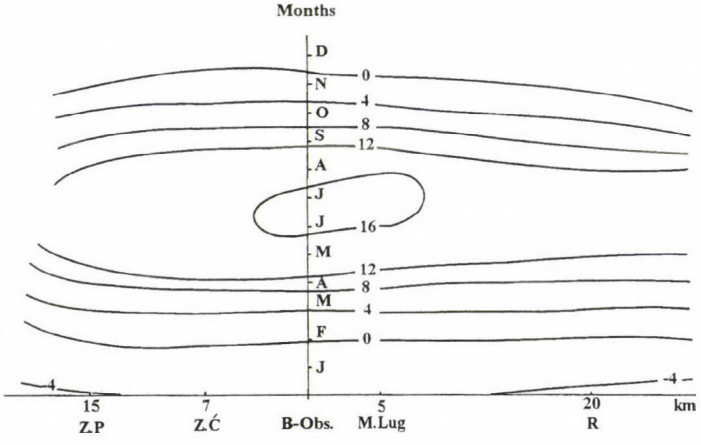

Fig. 4. Time-space section of the mean minimum temperature (°C).

Table 3. Minimum mean monthly temperature differences between the city and the surroundings (°C)

Temp. differ.	Jan	Feb	Mar	Apr	May	Jun	Jul	Aug	Sep	Oct	Nov	Dec	Year
ΔT_{s-r}	1.9	2.0	2.3	2.5	3.0	2.5	3.0	2.7	3.3	3.2	1.3	2.3	2.5
ΔT_{s-s}	1.3	2.2	1.6	1.7	2.0	1.2	2.3	2.3	1.4	15	1.0	1.1	1.8
ΔT_{u-r}	1.5	2.0	1.7	2.5	3.4	3.3	3.6	3.3	3.8	3.7	3.0	1.8	2.8
ΔT_{u-s}	1.9	1.6	1.9	2.2	1.5	1.6	2.2	1.0	1.9	1.1	2.0	1.0	1.6

Examination of the effect of urban heat island on urban precipitation is continued by using minimum temperature differences and precipitation differences from choice urban-rural pairs of stations during the period of strong industrialization in that part of the Belgrade area. The chosen urban-rural pairs of stations are: (a) Belgrade – Radmilovac (with minimum annual precipitation difference), (b) Zemun Ćukovac – Zemun Polje (with mean annual precipitation difference) and (c) Botanička Bašta – Besni Fok (with maximum annual

precipitation difference). The obtained results, represented on *Figs. 5a, b* and *c*, indicates that there are insignificant correlations between urban-rural differences in monthly total precipitation and mean minimum monthly temperatures i.e., that urban heat island (shown in Fig. 4) has no effect on increase of precipitation in strong urban zone of the Belgrade area. It might be concluded that the direct thermal effect on increase in urban precipitation is small and that the other effects as increase of nuclei concentration in urban atmosphere from anthropogenic activities and cloud dynamics are dominant.

Table 4. Seasonal precipitation differences ΔP (mm) between urban-rural pairs of stations (numbers 5, 6, 7, 10, 13, 15, 16, 18, 19, 20, 34 and 44 are related to stations assigned in Table 1)

ΔP (mm)	Winter	Spring	Summer	Autumn	Annual value (mm)	%
5-34	9.8	3.4	12.5	4.9	30.6	4.6
7-6	27.1	37.4	29.9	19.3	113.7	19.1
10-20	19.6	8.6	7.2	7.8	43.2	6.2
15-13	30.6	19.3	35.4	9.9	95.2	15.5
16-44	13.6	27.2	5.1	6.9	52.8	8.5
18-19	22.0	13.7	10.0	20.4	66.1	10.5
Average	**20.4**	**18.3**	**16.7**	**11.5**	**66.9**	**10.8**

4. Conclusions

Precipitation stations at the west edge of the Belgrade area show 20 mm to 50 mm more precipitation than stations on the eastern border of Belgrade area in annual average, confirming that the direction southwest-northeast is the direction of decreasing of station elevations.

Monthly precipitation in the Belgrade urban area does not seem to follow the rule that urban precipitation is always higher than rural.

However, seasonal precipitation amounts are changed by the presence of the city. In autumn and winter Belgrade receives between 5 mm and 31 mm and in spring and summer between 3 mm and 37 mm more precipitation than the surrounding area. It is obvious that the average annual increase of precipitation in urban station is between 5 and 19% in comparison with adjacent rural stations of similar heights.

It seems to be most likely that any urban effects upon rainfall are related to cloud dynamical effects associated with the heat island and surface roughness.

Because there is a gap between existing and needed rainfall data (usually not provided by national weather services), an urgent need exists for further research on data acquisition by traditional (i.e. rain gauge) and modern methods (i.e. radar and satellites).

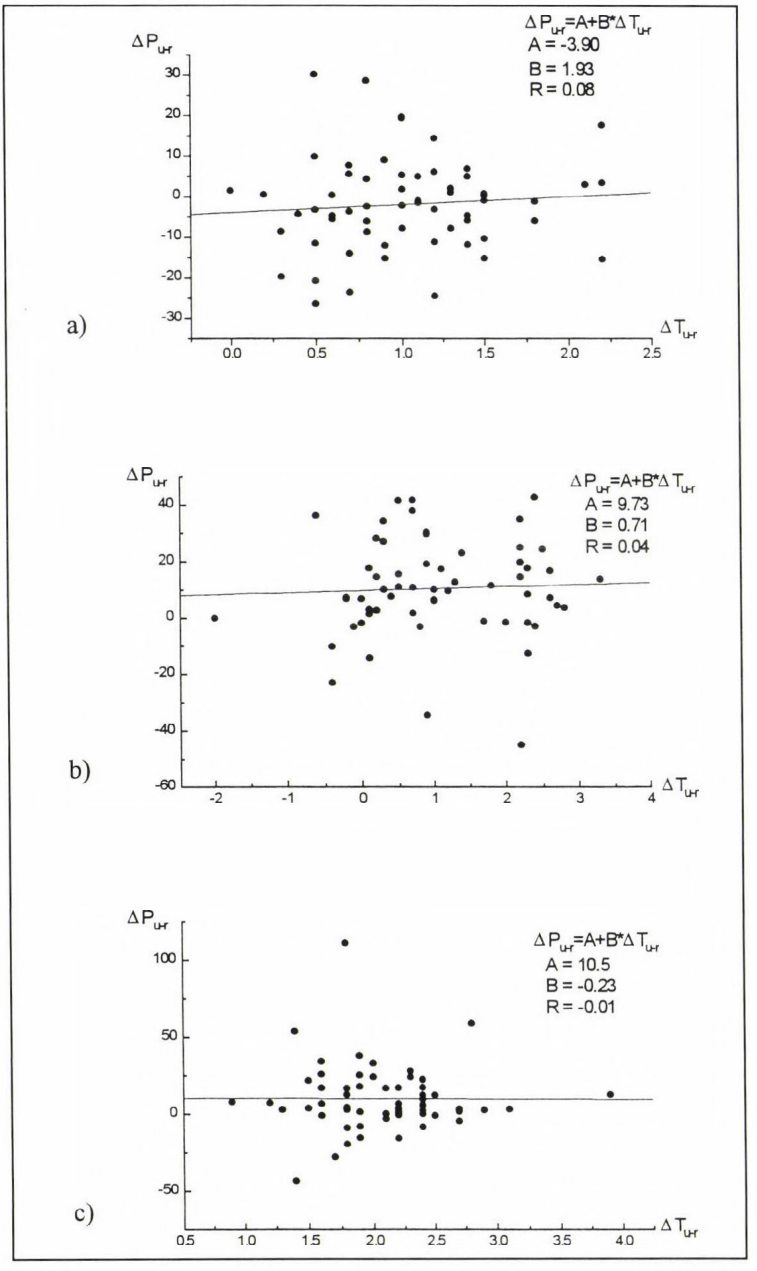

Fig. 5. Regression of differences in monthly total precipitation against differences in minimum monthly temperature between: (*a*) Belgrade (u) and Radmilovac (r) during the period 1987–1991; (*b*) Zemun Ćukovac (u) and Zemun Polje (r) and (*c*) Botanička Bašta (u) and Besni Fok (r) during the period 1987–1982.

References

Allerup, P., 1991: Statistical modelling of urban-scale precipitation data. *Atmos. Research 1-3*, 67-80.

Brazel, W.S. and *Balling, R.J.*, 1986: Temporal analysis of long term atmospheric moisture levels in Phoenix, Arizona. *J. Clim. Appl. Meteor. 25*, 112-117.

Chandler, T.J., 1976: *Urban Climatology and its Relevance to Urban Design*. Techn. Note, No. 149, WMO, Geneva.

Changnon, S.A., 1969: Recent studies of urban effects on precipitation in the United States. *Bull. Amer. Meteor. Soc. 50*, 411-421.

Ćurić, M. and *Janc, D.*, 1987: The effect of Belgrade on cloudiness during convective nights. *Bull. Serb. Meteor. Serv. 14*, 137-139.

Goldreich, Y., 1985: Urban topo-climatology. *Progress in Phys. Geog. 8*, 336-364.

Huff, F.A. and *Changnon, S.A.*, 1972: Climatological assessment of urban effects on precipitation at St. Louis. *J. Appl. Meteor. 11*, 823-842.

Isaac, G.A. and *Stuart, R.A.*, 1992: Temperature-precipitation relationships for Canadian stations. *J. Clim. 8*, 822-830.

Landsberg, H.E., 1981: *The Urban Climate*. Int. Geophys. Ser. 28, Academic Press, New York.

Oke, T.R., 1984: Methods in urban climatology. In *Applied Climatology*. Zurcher Geog. Schriften, Zurich, 19-29.

Oke, T.R., 1986: Urban climatology and the tropical city. In *Proc. Technical Conference on Urban Climatology and Its Applications with Special Regards to Tropical Areas*. WMO No. 652, Geneva, 1-25.

Sanderson, M., Kumanan, J., Tanguay, T. and *Schertzer, W.*, 1973: Three aspects of the urban climate of Detroit-Windsor. *J. Appl. Meteor. 12*, 629-638.

Thomas, M.K., 1971: A survey of the urban effect on the climates of Canadian cites. *Canadian Science*, No. 11-71, Environment Canada, Toronto.

Unkašević, M., 1991: Evidence of the urban heat island in Belgrade. *Beitr. Phys. Atmos. 1*, 55-63.

IDŐJÁRÁS

Quarterly Journal of the Hungarian Meteorological Service
Vol. 100, No. 4, October–December 1996

Analysis of harmattan dust over Accra, Ghana

K. Oduro-Afriyie and **K. Anderson**

Department of Physics, University of Ghana
Legon, Accra, Ghana

(Manuscript received 31 July 1995; in final form 13 June 1996)

Abstract—Harmattan aeolian dust from the Sahara desert which occurs in West Africa was monitored at Accra (5°32'N, 0°12'W) during the 1993/94 harmattan season. Dust deposition for 1993/94 harmattan season at Accra amounted to 4.8287×10^{-3} kg m^{-2}. Particle size analysis as well as X-ray fluorescence and neutron activation analyses were carried out on the harmattan dust. The particle size analysis indicated that the great majority of the particles deposited have a diameter above 1 μm with mean, mode and median diameters of 2.11, 2.00 and 1.73 μm, respectively. The deposition velocities, calculated by the Stokes formula, are 3.51×10^{-4}, 3.15×10^{-4} and 2.36×10^{-4} m s^{-1}, for these sizes respectively. X-ray fluorescence analysis of the dust showed the presence of the following elements, with the order of abundance as Fe > Ca > Cu > Ti > Zr > Pb > Sr > Rb > Y > Nb. In addition to these elements, neutron activation analysis also revealed the presence of elements: Na, K, Mn and Mg.

Key-words: harmattan dust, dry deposition, particle elemental composition.

1. Introduction

In West Africa, large quantities of dust particles are transported every year between November and March from the Sahara desert towards the Gulf of Guinea. The dust is transported by a cold dry wind, called the harmattan, which brings about one of the severest winter conditions and dust haze in the region (*Kalu*, 1977). The harmattan dust particles are kept air-borne for considerable length of time, and thereby produce a dusty atmosphere, which subsequently reduces visibility.

The harmattan dust has several source areas. One of such source areas is the Faya Largeau in Chad, off the western slope of the Tibesti-Massif (*Kalu*, 1977). According to *Wilson* (1971), the region responsible for the dusty atmosphere over West Africa is the Bilma-Faya Largeau area (see *Fig. 1*). Most of the dust settle over the coastal countries of West Africa (*Tiessen et al.*, 1991).

The Saharan dust also affects some parts of North Africa at certain periods of the year. For instance in summer, when the dust is essentially absent in West Africa south of the Intertropical Discontinuity (ITD), the trajectory of the dust changes to a westward direction to affect areas in the south western part of North Africa, such as Southern Algeria and Morocco, and further west to the Caribbean Islands across the Atlantic Ocean (*Prospero*, 1968).

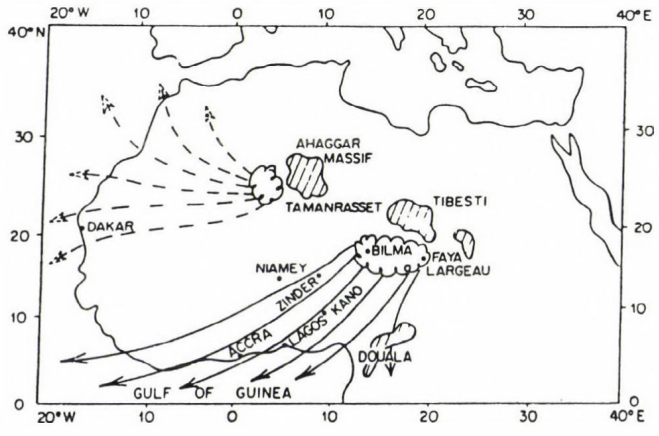

Fig. 1. Map of West Africa showing main source of harmattan dust; —— trajectory during winter; - - - trajectory during summer (*Kalu*, 1977).

The north-easterly winds blowing from the Sahara gives rise to high atmospheric turbidity and consequently, poor visibility in West Africa. The more turbid the atmosphere, the shorter the horizontal visibility (*Adeyefa* and *Adedokun*, 1991). Poor visibility, often caused by thick harmattan haze, frequently results in disruption of aviation schedules and sometimes aviation accidents over the West African sub-region. For example, because of the harmattan dust, visibility was only 300 m at Kano Airport, Nigeria, in the morning of 22 January, 1973, when 176 people lost their lives in the crash of a Jordanian airliner (*Hayward* and *Oguntoyinbo*, 1987).

Harmattan dust consists of atmospheric aerosol particles, and has some effect on climate. It interacts with solar radiation reaching the Earth's surface through scattering and absorption processes. It also affects the size distribution of cloud droplets and their optical characteristics (*Munn* and *Machta*, 1979).

Healthwise, harmattan brings an increase in viral diseases such as pneumonia, tuberculosis and meningitis. *Hayward* and *Oguntoyinbo* (1987) point out that outbreaks of cerebrospinal meningitis, irritation in the throat, cold symptoms and catarrh are associated with the onset of harmattan condition in West Africa.

Water bodies are polluted, and exposed foods become contaminated. These adversely affect the health and economy of a country.

On the positive side, harmattan dust may help to locally improve the structure and the micro-nutrient content of marginal soils (*Hayward* and *Oguntoyinbo*, 1987). It has been found to be the source of potassium and other basic materials in Volta shale soils in Northern Ghana (*Tiessen et al.*, 1991).

Adedokun et al. (1989) found in the harmattan dust the following major elements: Fe, Al, Ti, Si, Ca, Mg, Na and K with trace elements like Zn > Mn > Ni > Cu > Cr > Co > V > Li (in order of abundance) over Ile-Ife, Nigeria, during the harmattan seasons of 1983/84 and 1984/85. The mean and standard deviation of the particle sizes were 3.12 and 1.59 μm, respectively. They also found quartz, crodine and kaslinite as the main minerals in the harmattan dust.

The current study is intended to examine the physical and chemical characteristics of harmattan dust over Accra (5°32'N, 0°12'W) with a view to enhancing our knowledge on the harmattan dust in Accra. This would enable policy makers to tackle some of the problems associated with the harmattan dust.

2. Materials and methods

2.1 Sample collection

Harmattan dust samples were collected at five locations in Accra between December, 1993 and March 1994. These sites (*Table 1*) were chosen to give a fair representation of Accra. In order to avoid the intrusion of fugitive dust from local sources, the locations were sited far from any major road or bare land.

Table 1. Sites from which harmattan dust samples were collected

Site	Description
Atomic (AT)	Top of Radiation Protection Board building, Ghana Atomic Energy Commission, Kwabenya.
Legon (LEG)	Department of Physics, University of Ghana, Legon.
Meteo (MET)	Top of building in the weather observatory enclosure, Ghana Meteorological Services Department, Accra.
Airport (AP)	Top of a platform in the weather observatory enclosure, Kotoka International Airport.
Korle-Bu (KB)	Top of Medical School Laboratory building, Korle-Bu Teaching Hospital.

The dust was collected using locally constructed deposit gauges. Each deposit gauge consisted of a large funnel of cross-sectional area between 0.1052 and 0.1089 m^2. The nozzle of the funnel was fitted with a transparent polyethylene bag, which trapped the harmattan dust. Except at the Airport where sampling was done monthly because of stringent security measures, the dust was collected fortnightly at all sites.

For the particle size analysis, some of the dust particles were collected on clean glass slides mounted for 4 hours between 8.00 a.m. and 1.00 p.m. at the sampling sites.

2.2 Analyses

2.2.1 Particle size analysis

The particle size analysis was carried out with the aid of an Olympus CH2 optical microscope. The diameters of 5414 particles were measured.

Taking the density of a dust particle as 2.65×10^3 kg m^{-3} and the viscosity of air at 300K as 18.325×10^{-6} Ns m^{-2} (*Adedokun et al.*, 1989), the deposition velocities were computed for the various particle diameters using the well-known Stokes equation (see e.g. *Ludlam*, 1980).

2.2.2 Chemical analysis

An X-ray fluorescence spectrometer was used to determine quantitatively the chemical composition of the harmattan dust. The spectrometer was first calibrated against standards.

Dust samples collected from each site were put into pellets. Each side of a sample pellet was irradiated for 400 seconds. This was done to check the homogeneity of the sample.

Elemental analysis of the harmattan dust was also done using neutron activation analysis. This analytical technique was able to detect the elements with lower atomic numbers which the X-ray fluorescence analysis could not detect.

3. Results and discussion

Between 1.2015×10^{-3} kg m^{-2} and 10.8813×10^{-3} kg m^{-2} were collected at the five locations for 75 days. Deposition rates were low from December 22 to January 17, when the harmattan was relatively weak. The mean deposition and mean daily deposition rate for the entire harmattan season were 4.8287×10^{-3} kg m^{-2} and 0.0644×10^{-3} kg m^{-2} $(day)^{-1}$, respectively (*Table 2*).

Table 2. Dust collected at various sites

Station	Cross-sectional area of catchment funnel m^2	Total deposit $\times 10^{-3}$ kg	Deposit per unit $\times 10^{-3}$ kg m^{-2}	Deposit rate $\times 10^{-3}$ kg m^{-2} day^{-1}
MET	0.1052	0.1264	1.2015	0.0160
AT	0.1061	0.2276	2.1451	0.0286
KB	0.1070	0.7712	7.2075	0.0961
AP	0.1078	1.1730	10.8813	0.1451
LEG	0.1089	0.2949	2.7080	0.0361
	Mean	0.5186	4.8287	0.0644

3.1 Results of particle size analysis

Fig. 2 shows the mean frequency of deposited particles versus their diameter.

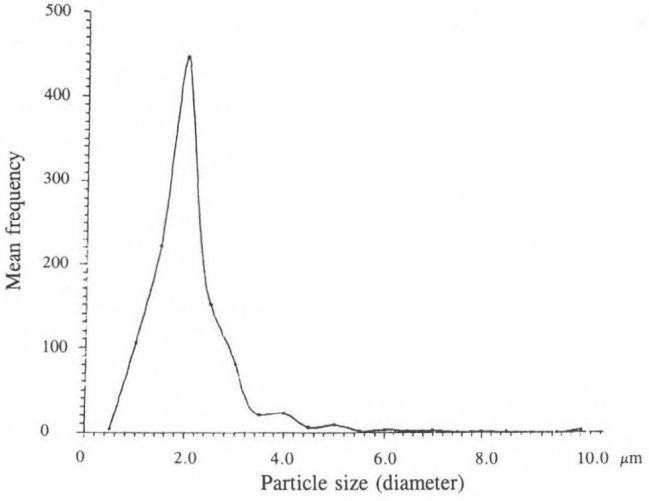

Fig. 2. Particle size distribution of harmattan dust over Accra.

The figure shows that:

(i) most of the particles (98.7%) have diameters less than or equal to 5.0 μm;

(ii) the mean diameter of the harmattan dust particles in Accra is 2.11 μm, with a standard deviation of 0.94 μm; 75.8% of particle diameters lie in the range (2.11 $\pm$ 0.94) μm;

(iii) the frequency distribution is close to a Gaussian distribution function, with mode at 2.00 μm. This value compares favourably with the 2.5 μm modal diameter obtained by *Adedokun et al.*, (1989) for Ile-Ife, Nigeria, which is nearer to the source region of the harmattan dust. The harmattan dust over Accra has a median particle diameter of 1.73 μm. This agrees with the findings of *El-Fandy* (1953) that, harmattan dust arriving in West Africa has particle diameter of 1.3 to 2.0 μm.

Bagnold's (1971) identification scheme on the deposited dust particles shows that 10.2% constitute haze. These have diameters ranging between 0.1 to 1.0 μm. The small percentage of particles in this size range among the deposited particles indicates that the majority of this range of particles remain suspended in the atmosphere for a long time. A typical diameter of about 0.50 μm can stay aloft for much longer periods, thereby causing atmospheric turbidity and poor visibility. They could only be washed out from the atmosphere by precipitation. These particles have diameters comparable to the wave-length of light (0.1 to 1.0 μm) and are therefore effective in scattering sunlight.

According to our observations, about 89.8% of the harmattan dust deposited have particle diameters greater than 1.0 μm. These are called coarse nuclei.

Head (1980) has shown that silt particles have diameters ranging from 2.0 to 6.0 μm, while clay particles have diameters less than 2.0 μm. Based on this classification, harmattan dust in Accra is composed of silt and clay in a relative quantity of 69.3% and 30.7%, respectively.

According to *Adefolalu* (1984) dust particles with diameters below 2 μm can reach the lungs of humans and bring about worsening conditions in respiratory ailments. 30.7% of the harmattan dust in Accra fall into this category. This might explain the outbreak of respiratory diseases in Accra during the harmattan season.

The particle diameters and their deposition velocities are presented in *Table 3*. The low values of the deposition velocities indicate that the particles do settle on surfaces at very slow rates. Their collision with human skins are therefore not felt.

3.2 Results of chemical analysis

X-ray fluorescence analysis of the dust particles revealed the presence of the following elements: Fe, Cu, Ti, Rb, Sr, Y, Zr, Nb and Pb. The dominant element detected was Fe and had an average value of 1.664% in abundance on mass basis. The least element in abundance was Nb with an average value of 5.5 ppm (*Table 4*). The order of abundance of the elements was Fe > Ca > Cu > Ti > Zr > Pb > Sr > Rb > Y > Nb.

The pattern of the elemental composition was the same for all the sampling sites. The high relative occurrence of Pb in the dust deposited at Legon might be attributed to exhaust fumes from the large concentration of vehicles on the campus, and which might have been trapped by the numerous trees.

Table 3. Particle diameters and computed deposition velocities of 1993/94 season of harmattan dust over Accra

Particle size	Diameter (μm)	Deposition velocity (ms^{-1})
Largest	10.00	7.87×10^{-3}
Mean	2.11	3.51×10^{-4}
Modal class	2.00	3.15×10^{-4}
Median	1.73	2.36×10^{-4}
Smallest	0.50	1.97×10^{-5}

Qualitative analytical results of the dust samples by neutron activation analysis showed the presence of the following elements: Ti, Na, K, Mn, Mg, Cu, Sr and Rb. These elements could not be quantified since the quantity of dust available at each site was less than 16×10^{-3} kg, which is the minimum amount required for such analysis.

The presence of these chemical elements in the harmattan dust, and the possibility of their deposition in the lungs and dissolution in the blood, might explain the high incidence of such ailments as cerebrospinal meningitis, irritation in the throat, colds and catarrh associated with harmattan in Accra. On the positive side, the presence of K and Na in the dust may help to improve the micro-nutrient content of the marginal soils in Accra.

Table 4. Elemental composition of harmattan dust at various sites (the relative quantities are expressed on mass basis)

Sample site	Ca ppm	Ti ppm	Fe %	Cu ppm	Rb ppm	Sr ppm	Y ppm	Zr ppm	Nb ppm	Pb ppm
KB	4800	2138	1.821	5982	16	42	12	175	7	98
AP	4121	2048	1.433	3582	13	30	9	133	8	64
LEG	7472	1653	1.704	4409	13	29	8	113	4	263
AT	3406	1503	1.697	1979	10	16	6	54	3	66
Mean	4949.8	1834.8	1.664	3969	13	29.3	8.8	118.8	5.5	122.8

4. Conclusions

The harmattan dust in Accra during the 1993/94 harmattan season was composed of 69.3% silt and 30.7% clay. The mean deposition of the dust during the entire sampling period was 4.8287×10^{-3} kg m^{-2}, with a mean deposition rate of 6.440×10^{-5} kg m^{-2} day^{-1}.

This study shows that 98.7% of the dust particles deposited have diameters less than or equal to 5.00 μm. The modal, mean and median diameters are 2.00, 2.11 and 1.73 μm, respectively. The particles have deposition or settling velocities of 3.15×10^{-4}, 3.51×10^{-4} and 2.36×10^{-4} m s^{-1} for the modal, mean, and median sizes, respectively.

Among the elements analyzed, the harmattan dust in Accra contained the following chemical elements: Fe > Ca > Cu > Ti > Zr > Pb > Sr > Rb > Y > Nb in order of abundance. Neutron activation analysis showed the presence of the following additional elements: Na, K, Mn and Mg.

Although the scope of this study was limited by the non-availability of X-ray diffractometer for mineralogical analysis, the results have thrown some light on the nature and chemical composition of harmattan dust in Accra.

Acknowledgements—The authors are grateful to the Director and staff of the Ghana Atomic Energy Commission, Accra, for the use of their X-ray spectrometer and neutron activation analyzer. They are also grateful for the hospitality offered to the first author by the International Centre for Theoretical Physics, Trieste, Italy where the final write-up was done during his Associateship visit in 1996; and to the Swedish Agency for Research Co-operation with Developing Countries for sponsoring the visit.

References

Adedokun, J.A., Emofurieta, W.O. and *Adedeji, O.A.*, 1989: Physical, mineralogical and chemical properties of harmattan dust at Ile-Ife, Nigeria. *Theor. Appl. Climatol. 40,* 161-169.

Adefolalu, D.O., 1984: On bioclimatological aspects of harmattan dust haze in Nigeria. *Arch. Met. Geoph. Biocl. Ser. B. 33*, 387-404.

Adeyefa, Z.D. and *Adedokun, J.A.*, 1991: Pyrheliometric determination of atmospheric turbidity in the harmattan season over Ile-Ife, Nigeria. *Renewable Energy 1*, 555-566.

Bagnold, R.A., 1971: *The Physics of Blown Sand and Desert Dunes*. Chapman and Hall, London.

El-Fandy, M.G., 1953: On the physics of dusty atmosphere. *Q. J. Roy. Meteorol. Soc. 79,* 284-287.

Hayward, D.F. and *Oguntoyinbo, J.S.*, 1987: *Climatology of West Africa*. Hutchinson Education, New Jersey.

Head, K.H., 1980: *Manual of Soil Laboratory Testing, vol. 1: Soil Classification and Compact Tests*. Pentech Press Limited, Plymouth, Devon.

Kalu, A.E., 1977: The African dust plumes; Its characteristics and propagation across West Africa in winter. In *Saharan Dust* (ed.: *A. Morales*). Wiley, New York.

Ludlam, F.H., 1980: *Clouds and storms*. University Park and London, Pennsylvania State Univ. Press.

Munn, R.E. and *Machta, L.*, 1979: Human activities that affect climate. *Proc. of the World Climate Conference,* Geneva, February, 1979.

Prospero, J.M., 1968: Atmospheric dust studies on Barbados. *Bull. Amer. Meterol. Soc. 49*, 645- 652.

Tiessen, H., Hauffe, H.K. and *Mermut, A.R.*, 1991: Deposition of harmattan dust and its influence on base saturation of soils in Northern Ghana. *Geoderma 49*, 285-299.

Wilson, I.G., 1971: Desert sand flow basins and a model for the development of ergs. *Geogr. J. 137*, 180-198.

BOOK REVIEW

Attila Kerényi: **Global Problems–Possible Solutions (General Questions of the Environmental Protection)** (in Hungarian with English summary). Mozaik Oktatási Stúdió, Szeged, Hungary, 1995, 383 pages.

A new book is published in the rich series of books on environmental protection. The book is warmly recommended to everybody who has any connection with environmental protection, deals with any topic of it, teaches it, or a member of any environmental movement, works for an environmental office in a council or he or she only is simply interested in the happening of our days.

We have the honour to Hungarian publishers for having published many translated books on environmental protection since the 70's. Lately, Hungarian authors have written too on the topic so the numbers of books concerning in the subject have grown into a small library. In these circumstances it is very hard to write a book that gives newer and more information than the earlier ones. Attila Kerényi fulfilled this requirement in many respects.

The book, 'General Environmental Protection' looks over the development of the earthly environment, the qualitative changes of it from the beginnings to nowadays. It displays the connection of the human being with its natural environment from the ancient time. The historical view and the system conception both characterise the chapters throughout the book. Logical argument and extremely many facts illustrate the deepest roots of the environmental problems that have grown global nowadays.

The author not only draws the problems. As the subtitle of the book signs too, he takes more care of the possible solutions than most of the earlier authors. From the most general principle of solutions to the most concrete solutions he presents many ways and real means on several areas of environmental protection.

The book redefines the basic environmental concepts and analyses their connections and relations. It deals with the action system of the environmental movement and emphasises the environmental tasks of different fields. The longest chapter presents the mutual connection between the human population and the environment as well the damaging effect of the production and consumption on environment. The author considers the action to slow the human demographic expansion and to produce energy with technology saving the environment, to be key factors. He discusses both topics in detail and gives real prospects on the future of atomic energy and recycling energy sources. The effect of mining, metal industry, transport, chemical industry and

agriculture are analyzed later. Alternatives are suggested for the prevention of the damaging effects of these activities.

The book contains the consequences of the different forms of consumption and offers methods to learn to live with less as an alternative. Besides the usage of home garbage and sewage we can find chapters on the connection of tourism and environment and sport and environment.

The author deals with those environmental damages which do not connect with the pollution directly such as deforestation, overfishing, overgrazing, the effect of the change in field usage, soil erosion, deflation and the adverse effect of secondary alkalisation in the soil. Afterwards, basic knowledge on environmental pollution and waste follows.

The sixth chapter reveals the human effects on the changing operation of the global earth system. The subtopics in this chapter are the following: climate change, desertification, thinning of the ozone layer, acidification of the environment, pollution of the oceans, damage and extinction of species.

The chapter on the basic principles of environmental protection is a novelty. These principles 'work like lighthouses on seaside helping too determine the right way'. Among the principles a few ones are defined at the first time in the book.

The chapters on the economics and legal regulation of environmental protection are written by *Tibor Szász* and *Gyula Bándi*, respectively. A short chapter on chemical industry is the work of *Jenő Borda*.

In the last chapter, the author draws attention to the development of the environmental awareness. It is worth citing the last sentence: 'Considering all the facts we mentioned here on environmental education and training, we can be certain that the future of our environment depends on what is happening at schools'.

Summarising, the real worth of the book is the followings: presents the problems without extremity, gives many alternatives for solutions, it is highly systematised, informative, wide scaled and it has mind changing approach. The book can serve as a manual too, because it has a good index of about 1500 words and a glossary to understand the basic notions.

We are sure that the book is one of the most remarkable Hungarian books published on environmental protection lately (by Mozaik Oktatási Studió, Szeged).

Imre Berki

NEWS

IDŐJÁRÁS Centenary Session

This issue of IDŐJÁRÁS (No. 4, 1996) closes the 100th volume of the journal. Previously (No. 1–3) a brief summary of the 99-year history reminded the readers of this special event.

For more than a quarter of a century, every year, the Hungarian meteorological community has been holding a two-day session under the title: Meteorological Scientific Days (MSD). In 1996 the second part of MSD was dedicated to IDŐJÁRÁS as its Centenary Session. For this occasion *Dr. Iván Mersich,* President of the Hungarian Meteorological Service, invited the 14 foreign members of the Editorial Board of IDŐJÁRÁS. From them nine colleagues came to Budapest to attend the meeting:

H.-W. Georgii, Germany
D. Möller, Germany
F. Neuwirth, Austria
S. Panchev, Bulgaria
J. Pretel, Czech Republic
A. Renoux, France
D. Spänkuch, Germany
D. A. Wilhite, USA
D. Závodsky, Slovakia.

Best wishes were expressed in writing for the other members and for the future of the journal by *B. Fisher* (U.K.) and *K. Ya. Kondratyev* (Russia), and also by *P. Brimblecombe* (U.K.), executive editor of the journal Atmospheric Environment.

The speakers of the Centenary Session and the titles of their presentations were the followigs:

Ernő Mészáros, academician, professor of Veszprém University (Hungary), he teaches environmental sciences. He was editor-in-chief of the journal for 15 years. **The role and tasks of IDŐJÁRÁS.**

Tibor Braun, professor of Eötvös Loránd University of Budapest, on the one hand he teaches and investigates chemistry, on the other hand he is a very well known scientometrist of the Library of the Hungarian Academy of Sciences. **The demography of scientific journals**.

Donald A. Wilhite, professor of University of Nebraska, Lincoln, USA, and director of Drought Research Center. **International nature of drought monitoring, response and mitigation efforts.**

Stoycho Panchev, professor of Clement Okhridsky University of Sofia, he teaches dynamic meteorology. **Nonlinear dynamics, chaos theory and applications as presented in meteorological journals and university education.**

Dietrich Spänkuch, scientist with the German Weather Service in Potsdam. He deals with IR atmospheric sounding. **UV radiation forecast and ozone monitoring at the Meteorological Observatory Potsdam**.

Dusan Závodsky, chief scientist of the Slovak Hydrometeorological Institute, president of the Slovak Meteorological Society. He deals with air chemistry. **Cooperation of Slovak and Hungarian meteorologists**.

The full session has been recorded on VIDEO tape.

At the end of the Centenary Session a reception was given by *Dr. Iván Mersich*. He expressed his thanks to all the contributors and editors for the past 100 years and invited the international and Hungarian meteorological community to help in the operation of IDŐJÁRÁS for the next 100 years!

G. Major

IDŐJÁRÁS

VOLUME 100 * 1996

BUDAPEST, HUNGARY

AUTHOR INDEX

TABLE OF CONTENTS

I. Papers

II. Book review

III. News

IV. Subject index

The asterisk denotes book reviews or news